

102

THOMAS - SSS

FRACTURE TOUGHNESS OF AFT (LOX)
DOME MERIDIAN WELDS FOR THE SATURN S-IVB

DAC 62138



N70-75572

FACILITY FORM 602

(ACCESSION NUMBER)

79

(PAGES)

CR-112339

(NASA CR OR TMX OR AD NUMBER)

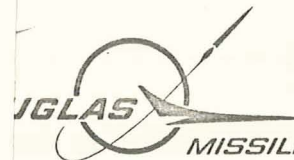
(THRU)

none

(CODE)

(CATEGORY)

T-U-S-IVB - M-68-1206



MISSILE & SPACE SYSTEMS DIVISION


67

FRACTURE TOUGHNESS OF APT (LOX)
DOME MERIDIAN WELDS FOR THE SATURN S-IVB

DOUGLAS REPORT DAC 62138
DATE: 8-23-68

Prepared by: R. A. Rawe, D. E. Schwab,
R. S. Wroth and H. Taketani
Metallics Branch

Prepared for:
National Aeronautics and
Space Administration
Huntsville, Alabama
Contract NAS 7-101


Approved by: G. V. Bennett
Branch Chief, Metallics
Materials & Methods -
Research & Engineering

Catalog No. PDL 86945

ACKNOWLEDGEMENT

The authors wish to recognize the valuable assistance and advice provided to them during the period of this program by a number of individuals, particularly, G. V. Bennett, E. V. Wysocki, P. W. Trester, J. L. Cook and D. A. Eitman.

ABSTRACT

A test program was undertaken to determine the effects of cracks in the meridian welds of the SATURN S-IVB Aft (LOX) Dome. Panels of 2014-T6 were fabricated on production and on laboratory MIG welding fixtures using 4043 filler wire. The panels, containing artificial cracks in the welds, were tested at 70°F and at -320°F. Some panels, tested at -320°F, were loaded to a proof stress level at 70°F prior to testing. Both static and cyclic tests were performed. The effects of repair welding, panel width, and crack size were examined. It was found that partial-thickness cracks extend on rising load, a phenomenon promoted by the presence of bending. Very deep partial-thickness cracks can extend and penetrate the thickness causing a leak. It was concluded that the current proof test of the S-IVB LOX tank, followed by post-proof inspection and leak testing of the welds, provides adequate assurance that the LOX dome is safe under operating conditions.

TABLE OF CONTENTS

	<u>Page</u>
ABSTRACT	11
LIST OF FIGURES	v
LIST OF TABLES	vii
LIST OF SYMBOLS	viii
1.0 <u>INTRODUCTION</u>	1
2.0 <u>PROCEDURE</u>	2
2.1 <u>Welding</u>	2
2.2 <u>Specimen Design and Preparation</u>	5
2.3 <u>Notching and Precracking</u>	8
2.4 <u>Crack Measurement</u>	11
2.5 <u>Testing</u>	11
2.6 <u>Data Computation</u>	16
2.6.1 Partial-Thickness Crack Tests	16
2.6.2 Through-Thickness Crack Tests	21
3.0 <u>RESULTS</u>	21
3.1 <u>Weld Land Specimens</u>	21
3.1.1 Tensile Properties of Weld Lands	22
3.1.2 Bending in Weld Lands	22
3.1.3 Static Fracture Tests of Weld Lands	27
3.2 <u>Uniform Thickness Specimens</u>	32
3.2.1 Tensile Properties of Meridian Welds	32
3.2.2 Static Fracture Tests of Meridian Welds	36
3.2.3 Cyclic Flaw Growth Tests of Meridian Welds	43

TABLE OF CONTENTS (Cont'd)

	<u>Page</u>
4.0 <u>DISCUSSION OF RESULTS</u>	49
4.1 <u>Flaw Growth in Weld Lands</u>	49
4.2 <u>Effect of Test Temperatures, Weld Type and Prior Proof Testing on K_{Ic}</u>	50
4.3 <u>Use of Net Section Stresses</u>	51
4.4 <u>Leak-Before-Burst</u>	51
4.4.1 Leak Modes	51
4.4.2 Evidence of Stable Leak Conditions	54
4.5 <u>Assessment of Safety of LOX Dome Weldments</u>	55
5.0 <u>CONCLUSIONS</u>	59
6.0 <u>RECOMMENDATION</u>	63
7.0 <u>REFERENCES</u>	63
APPENDIX A -- NONDESTRUCTIVE METHOD OF DETERMINING FLAW DEPTH	64

LIST OF FIGURES

<u>Figure No.</u>		<u>Page</u>
1	Tooling and Joint Details for Laboratory Welds Used in Weld Land Tests	3
2	SATURN S-IVB Fixture for Seam Welding Gore Segments for Fwd Hydrogen, LOX and Common Bulkhead Domes	4
3	Pin-Loaded Tensile Specimen	6
4	Weld Land Specimen	7
5	Six-Inch Wide Uniform Thickness Specimen	9
6	Twelve-inch Wide Uniform Thickness Specimen	10
7	Eccentric and Symmetric Loading	15
8	Effect of Width on Ratio of Gross Stress to Net Stress in a Cracked Panel	18
9	Bending in 5:3 Weld Land with Interior Surface Notch	24
10	Bending in 5:3 Weld Land with Exterior Surface Notch	25
11	Flaw Growth Due to Bending During 70°F Proof Test of Specimens 7-4 and 7-6	29
12	Flaw Growth Due to Bending During 70°F Proof Test of Specimens 7-1 and 7-3	30
13	Flaw Growth Due to Extra-Eccentric Proof Test at 70°F	31
14	Flaw Growth in Weld Lands During Eccentric and Symmetric Proof Testing	33
15	Stress Vs Flaw Size for Partial-Thickness Crack Virgin and Repair Welds in Uniform Thickness Panels Tested at 70°F	38

LIST OF FIGURES (Cont'd)

<u>Figure No.</u>		<u>Page</u>
16	Stress Vs Flaw Size for Partial-Thickness Crack Virgin and Repair Welds in Uniform Thickness Panels Tested at -320°F After Proof Testing at 70°F	39
17	Stress Vs Flaw Size for Partial-Thickness Crack Virgin and Repair Welds in Uniform Thickness Panels Tested at -320°F Without Prior Proof Testing	40
18	Flaw Growth in Uniform Thickness Welds During Proof Testing	41
19	Effect of 70°F Proof Test on Crack Surface Appearance and Growth in Partial-Thickness Crack Specimens (Gaps)	42
20	Stress Vs Critical Length for Through-Cracked Virgin Welds in Uniform Thickness Panels Tested at 70°F	47
21	Scribed 12-inch Wide Through-Thickness Crack Specimen	48
22	Verification of the Use of Net Stress for 6-inch Wide Panels	52
23	Data Bands for All Static Tests of Partial-Thickness Crack Specimens	56
24	Effect of Cracks on S-IVB LOX Dome Meridian Welds at Proof and Operating Stresses	57
A-1	MRA Data for Notched and Cracked Virgin and Repair Weld Panels	65

LIST OF TABLES

<u>Table No.</u>		<u>Page</u>
1	Test Program	12
2	Results of Weld Land Tensile Tests	23
3	Weld Land Strain Gage Data	26
4	Weld Land Static Fracture Toughness Test Results	28
5	Tensile Properties of Uniform Thickness Welds at 70°F and -320°F	34
6	Tensile Properties of Uniform Thickness Welds at -320°F After Proof Testing at 70°F	35
7	Static Fracture Test Results for Uniform Thickness Partial-Thickness Crack Specimens	37
8	Results of Static Tests on Welded Through-Cracked Specimens	44
9	Uniform Thickness Cyclic Flaw Growth Tests	45
10	Summary of Effects of Cracks in S-IVB LOX Dome Meridian Welds	60

SYMBOLS

A_c	= Effective area of crack
A_g	= Gross cross-sectional area of test section = width X thickness
A_n	= Net cross-sectional area of test section = $A_g - A_c$
a_i	= Initial crack depth (before proof testing)
a_p	= Final crack depth after proof testing
B	= Thickness of flawed region (e.g., shaved weld)
$2c_i$	= Initial crack length (before proof testing)
$2c_p$	= Final crack length after proof testing
EDM	= Electrical discharge machining
E_t	= Elastic (Young's) Modulus in tension
K_c	= Critical stress intensity for plane-stress conditions based on ℓ_c
K_{CN}	= Critical stress intensity for plane-stress conditions based on ℓ_o
K_I	= Plane-strain stress intensity
K_{Ic_g}	= Plane-strain fracture toughness based on $\sigma_{gf} = 1.1 \sigma_{gf} \sqrt{\pi a_p/Q_{gf}}$
$K_{Ic(net)}$	= Plane-strain fracture toughness based on $\sigma_{nf} = 1.1 \sigma_{nf} \sqrt{\pi a_p/Q_{nf}}$
ℓ_c	= Length of through-crack immediately prior to fracture
ℓ_o	= Length of initial through-crack (prior to testing)
MRA	= Magnetic Reaction Analyzer (eddy-current device)
P	= Load at fracture
Q_{gf}	= Crack shape parameter based on gross fracture (or cyclic) stress and yield strength at test conditions
Q_{nf}	= Crack shape parameter based on net fracture (or cyclic) stress and yield strength at test conditions
S/P	= Single pass
W	= Specimen width
σ_g	= Gross section stress = Load/ A_g
σ_{gf}	= Gross fracture strength = Fracture Load/ A_g

SYMBOLS (Continued)

σ_{gp}	= Gross proof stress = Proof Load/ A_g
σ_n	= Net section stress = Load/ A_n
σ_{nf}	= Net fracture strength = Fracture Load/ A_n
σ_o	= Operating stress
σ_{np}	= Net proof stress = Proof Load/ A_n , using a_p and $2c_p$
$\sigma_y = F_{ty}$	= Yield strength
ϕ	= Geometric crack shape correction factor

1.0 INTRODUCTION

This testing program was initiated to determine the ability of the current proof test to detect pre-existing defects in the meridian welds of the aft (LOX) dome of the SATURN S-IVB. Artificial defects of various sizes were generated in welded 2014-T6 panels and the panels were loaded under conditions simulating proof testing and flight of the LOX tank. Production welding procedures for the aft dome meridian welds were employed in preparing the test panels. The results of the tests were analyzed to predict the minimum defect sizes which cause crack propagation to occur at stresses corresponding to proof and flight loading.

Proof test of the LOX tank is conducted by hydrostatic pressurization with water. At maximum proof pressure the meridian weld experiences a calculated stress of 18.6 ksi normal to the weld. Panel tests simulating proof conditions were therefore performed at room temperature. During flight, the meridian weld can experience a maximum stress of 25.2 ksi at the temperature of liquid oxygen, -298°F . Panel tests simulating flight conditions were conducted in liquid nitrogen at -320°F .

2.0 PROCEDURE

2.1 Welding

Weldments from which the several types of test specimens were excised were prepared both in the Welding Development Laboratory and in the manufacturing departments. In either case welding procedures and parameters conformed to the process detailed in specification DPS 14052. Briefly, this consisted of a square butt, single pass, MIG weld in 2014-T6 aluminum alloy sheet using 4043 alloy filler metal. After welding, the weld metal reinforcement and underbead penetration were removed flush with the parent metal surfaces by shaving and sanding. All welds were inspected by visual, penetrant, and X-ray methods to the quality requirements of DPS 14052. Only those welds meeting these requirements were used to fabricate test specimens.

All of the laboratory welds were used in the weld land phase of the investigation. These were 30-inch long by 15-inch wide welded panels in 0.221-inch thick sheet. The material was chemically milled prior to welding to a membrane thickness of 0.133-inch starting 1-9/16-inches from the butt joint interface. Welds were made both from the chem-milled side of the joint, and from the flat side according to the particular need of the specimens to be tested. Virgin welds only were prepared in this phase of the study. A cross-section drawing of the weld joint and tooling details for these laboratory weldments is shown in Figure 1.

Flat panel weldments for uniform thickness tests were prepared in production tooling used for making SATURN S-IVB LOX dome meridian welds. The tool is shown in Figure 2. This fixture, which is spherically contoured, was used to weld flat panels. In order to insure that joint

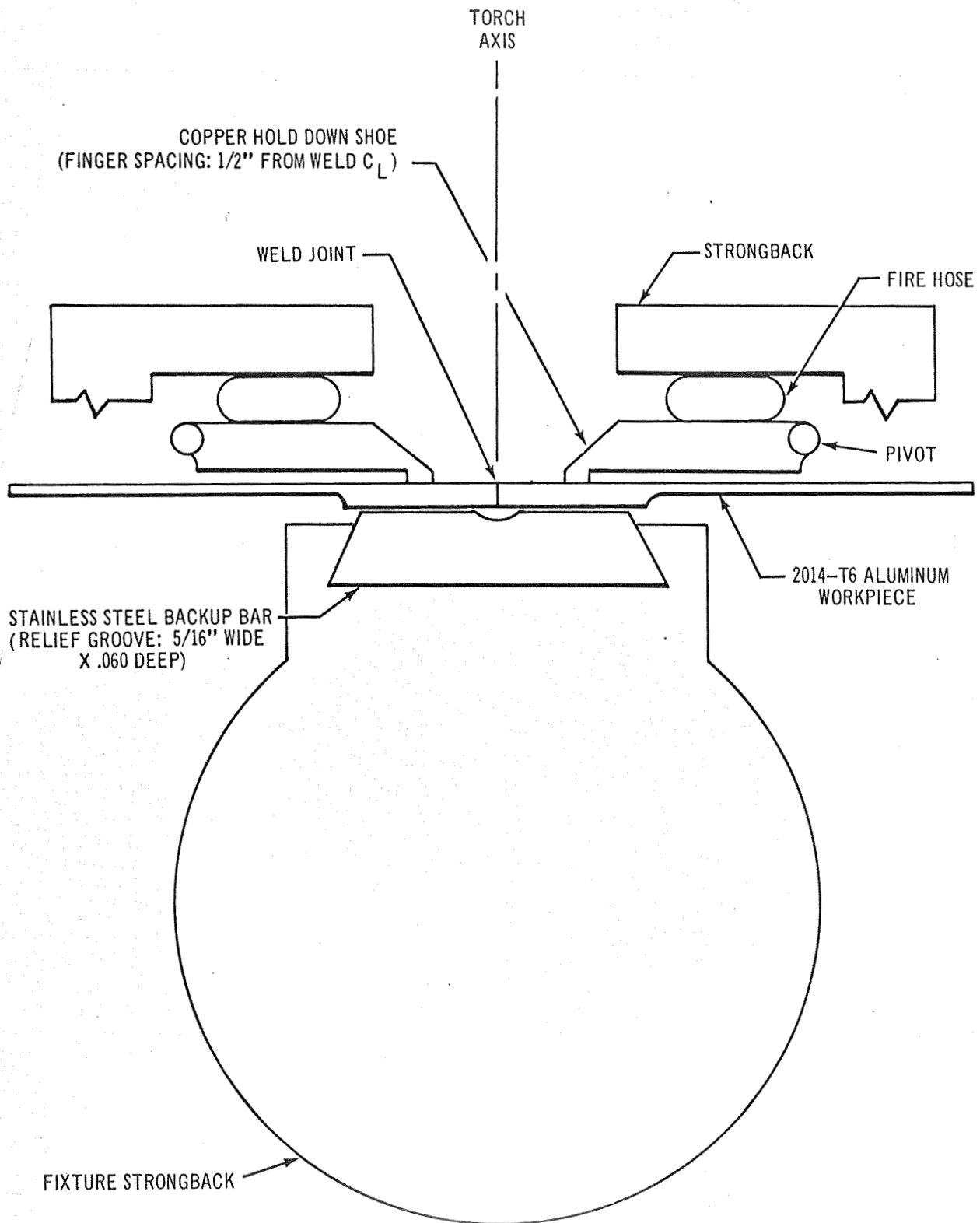


Figure 1. Tooling and Joint Details for Laboratory Welds Used in Weld Land Tests.

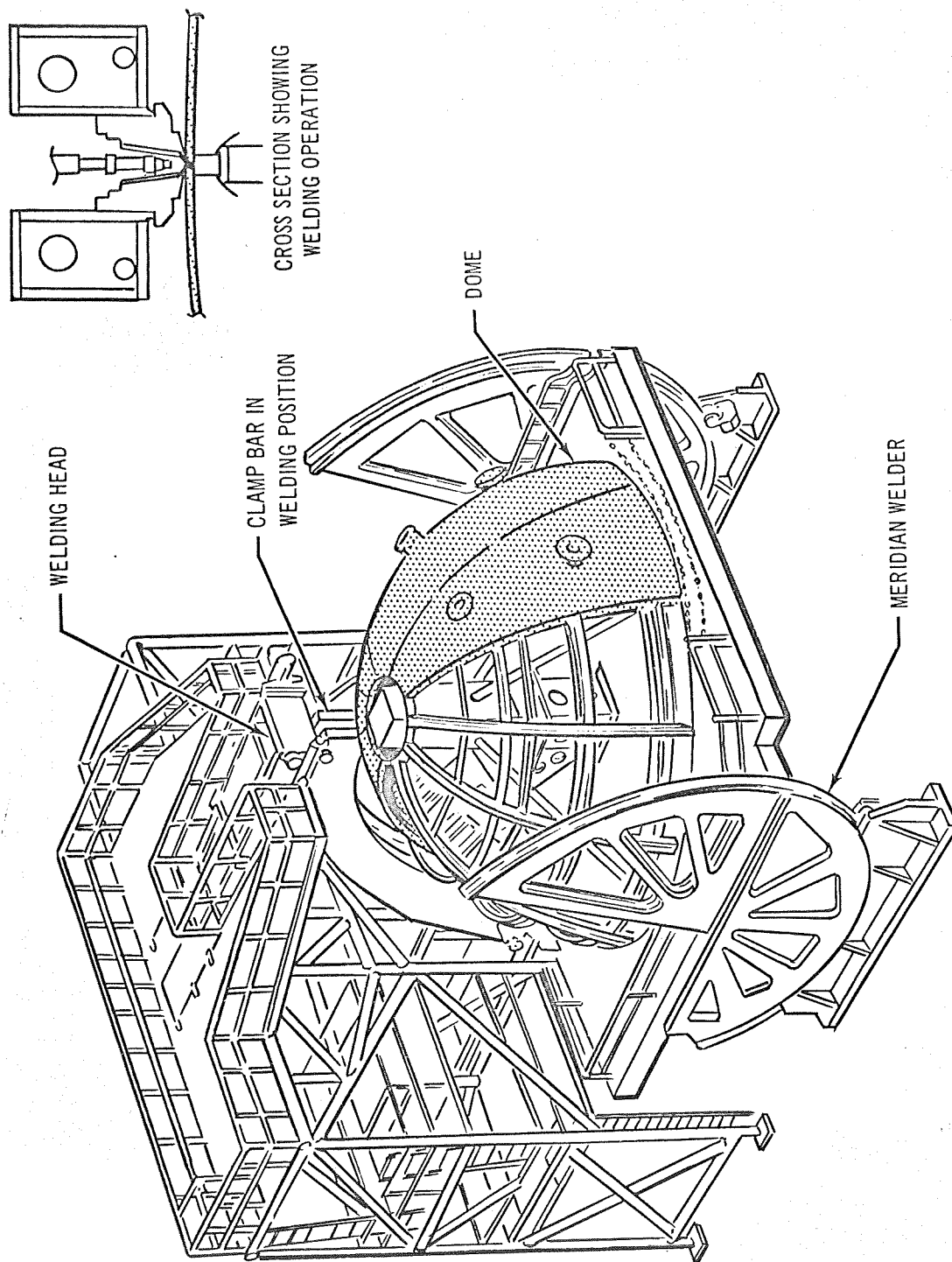


Figure 2. Saturn S-IVB Fixture for Seam Welding Gore Segments for Fwd Hydrogen, Lox and Common Bulkhead Domes

fit-up variations did not exceed process specification limitations due to compound bending of the flat panels, it was necessary to limit weld length to 30-inches, and the panel width to 14-inches in the 0.190-inch thick sheet material. A series of such weldments were prepared to provide the necessary number of test specimens. Both virgin and double-repaired welds were made. The sequence for each was as follows:

Virgin: weld + shave

Double Repair: weld + shave + weld + shave + weld + shave

Weld panels for extra-wide (12-inch) and extra long (36-inch) uniform thickness specimens were prepared by extending the width of the 14-inch wide panels to 36 inches. To do this, 11-inch extensions were welded to each side of two 14-inch wide virgin weld panels. Welding of the 14-inch wide panels was performed on the LOX dome fixture and welding of the extensions was done in the Welding Laboratory. Extension welds were made using two-pass, square butt MIG welding with one pass from each side of the joint in order to achieve maximum joint efficiency with minimum distortion.

2.2 Specimen Design and Preparation

Figure 3 illustrates the configuration of the tensile specimen used for determination of joint and weld-metal mechanical properties. Fracture toughness specimens for tests of weld joints with the land were 4-inches wide by 15-inches long and contained a centered weld perpendicular to the long dimension, as shown in Figure 4. The majority of tests on

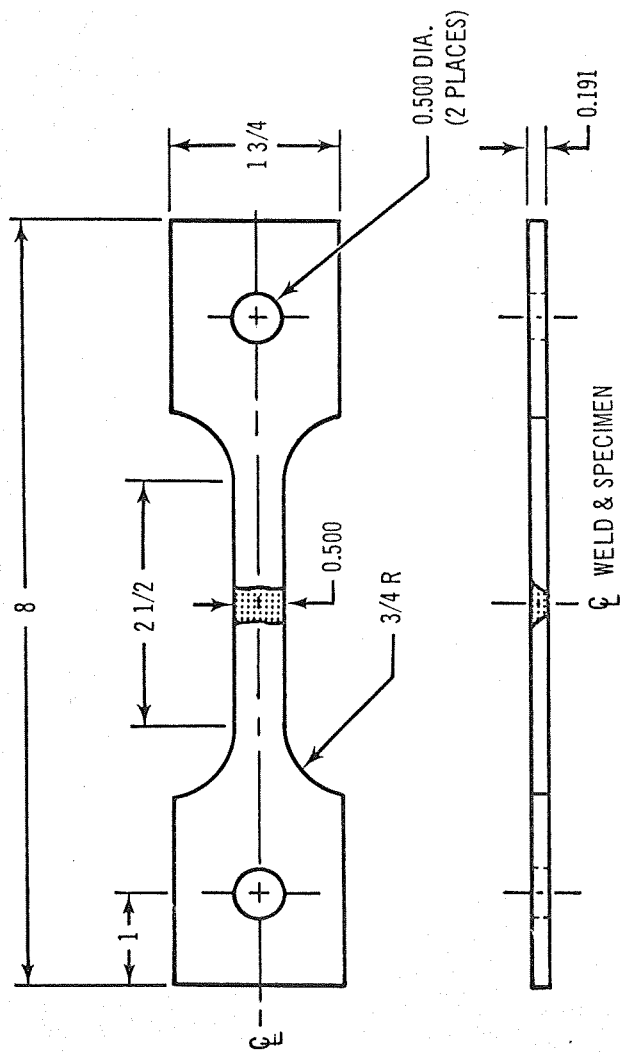


Figure 3. Pin-Loaded Tensile Specimen

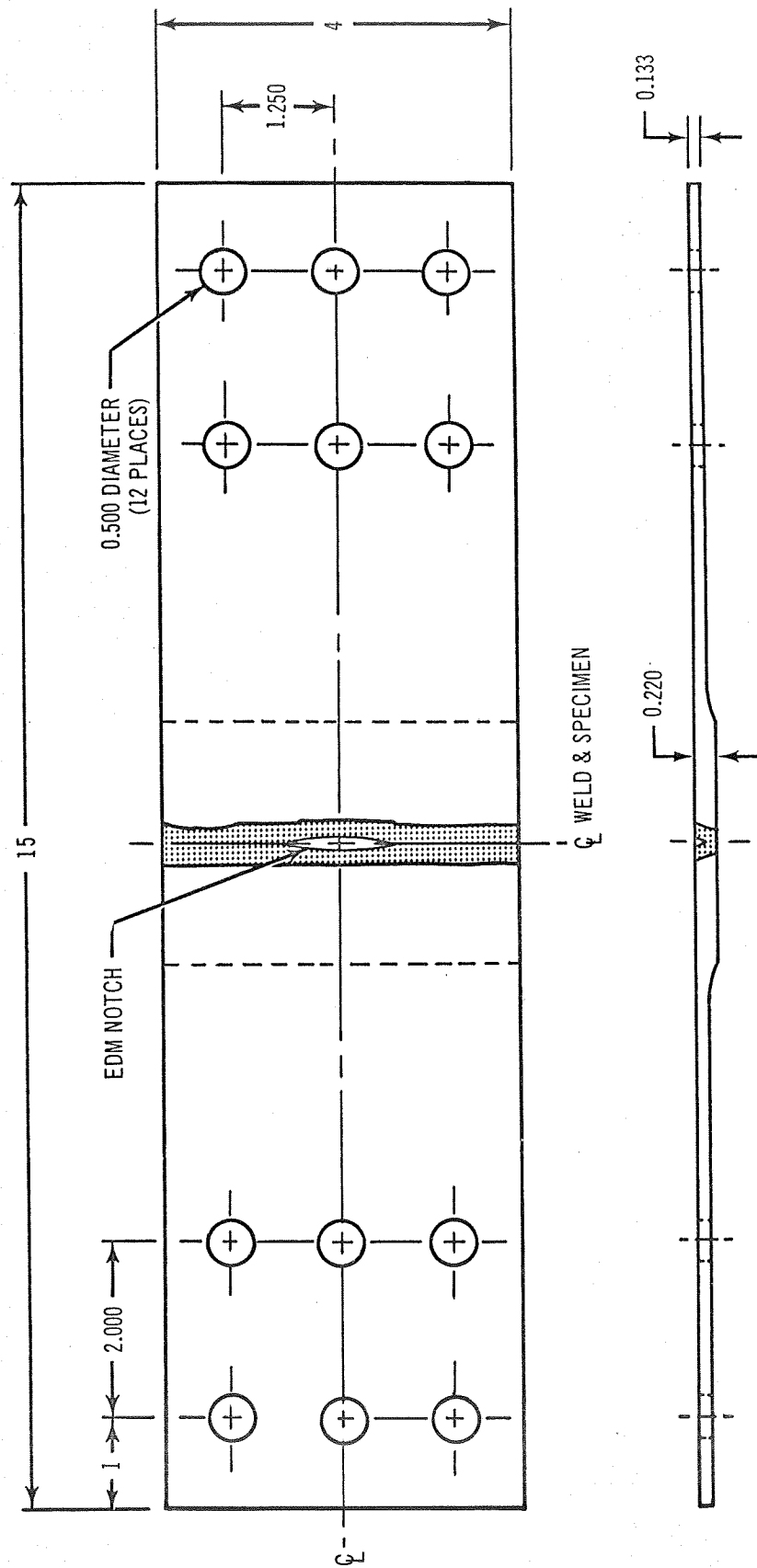


Figure 4. Weld Land Specimen

uniform-thickness specimens (no weld land) was performed using specimens 6-inches wide by 14-inches long, as shown in Figure 5. Several uniform-thickness specimens, tested to evaluate effects of added width and through-cracks, were 12-inches wide by 36-inches long, as shown in Figure 6.

All specimens were permitted to remain at room temperature a minimum of 12 days prior to testing to ensure that the natural aging process, which takes place in the weld at room temperature, was essentially complete. Certain 6-inch wide specimens were exposed to 160°F for three days after proof testing to simulate the insulation cure cycle used for the S-IVB stage.

2.3 Notching and Precracking

In order to provide the desired variety of crack sizes in the fracture toughness specimens, both flexure and axial tension-tension fatigue were employed. An EDM notch was located in the center of the weld with the long dimension of the notch being perpendicular to the long axis of the fracture toughness specimens. The notches were extended using low-stress fatigue. The cycles required to grow the crack varied with the desired crack size. Typical values ranged from 20,000 to 100,000 cycles.

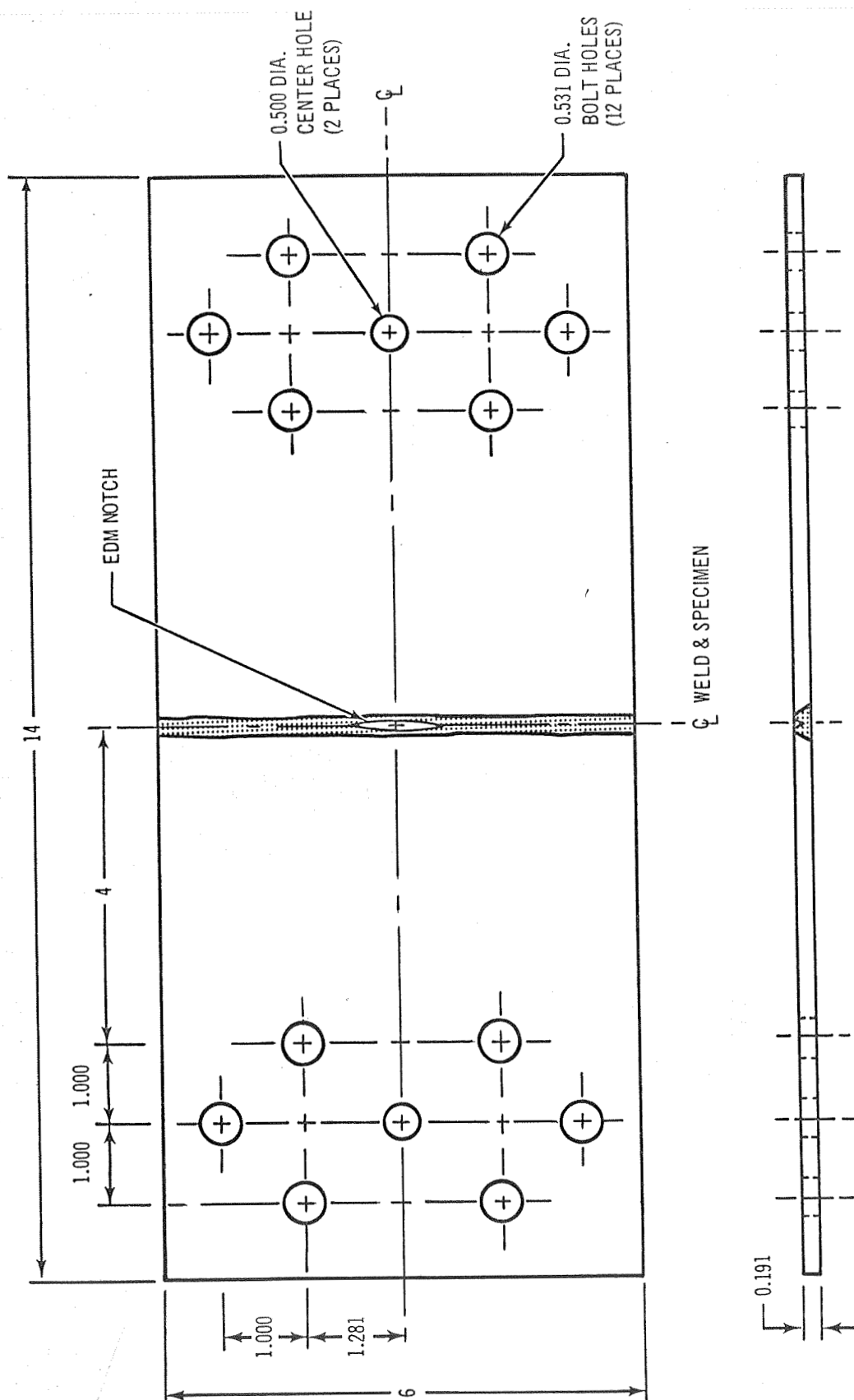


Figure 5. Six-Inch Wide Uniform Thickness Specimen

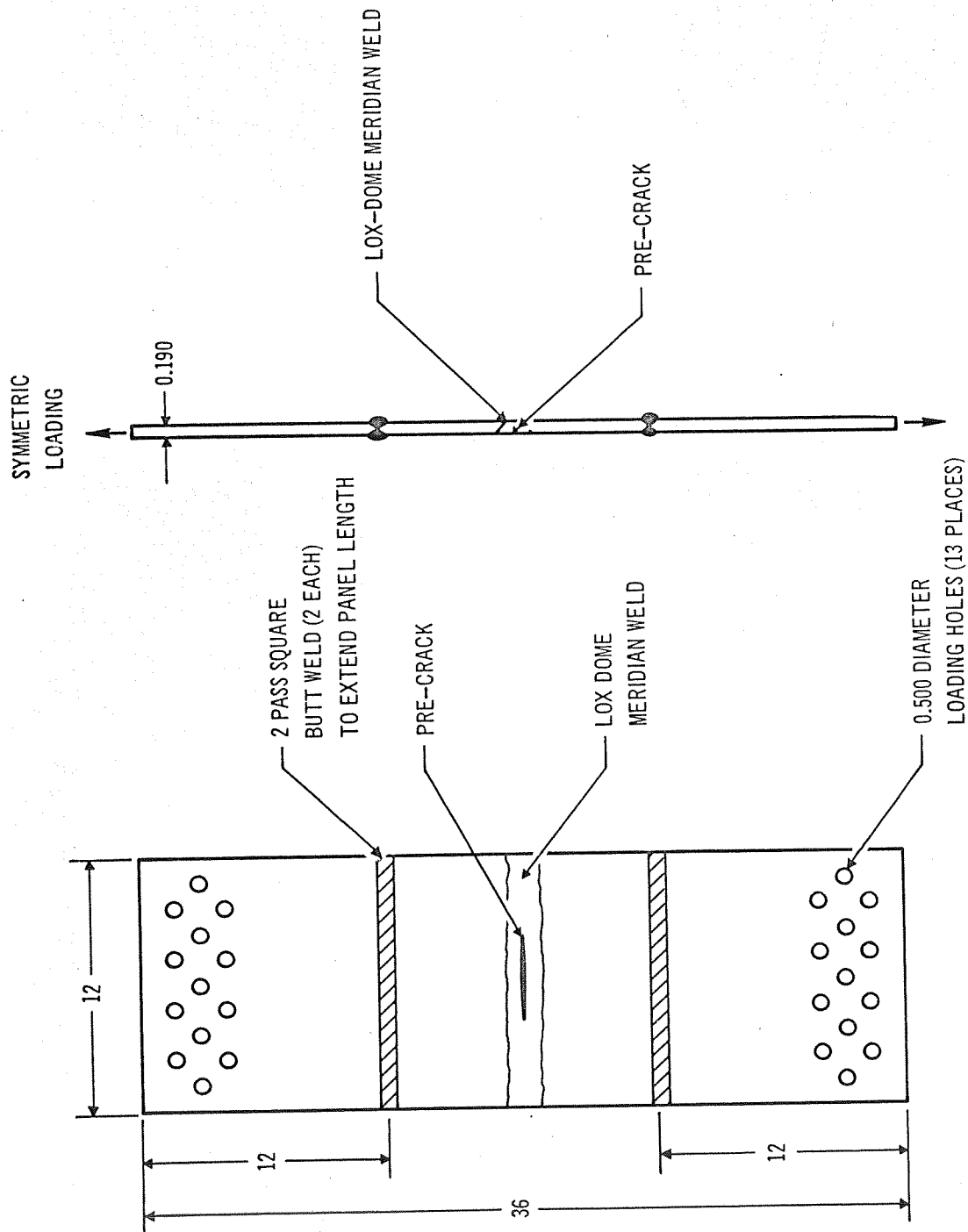


Figure 6. Twelve-Inch Wide Uniform Thickness Specimen

2.4 Crack Measurement

EDM notch, pre-crack, and final crack dimensions, depth (a) and length ($2c, l_0$) were determined after testing directly from the fracture surfaces. The method consisted of mounting the fractured specimen in a cross-slide having a micrometer screw adjustment. The fracture surface was viewed through a stereo microscope having ten to forty power magnification. The specimen was traversed across the field of vision which included a cross-hair sight, and micrometer readings were taken at points of demarcation between specimen edge, notch edge, and crack edge. Both fracture surfaces of each specimen were measured and the readings for each were compared to establish the average. Both length and depth measurements were made in the same manner.

The above described method of measuring cracks could be performed only after specimen failure. An attempt was made to establish a non-destructive criteria for determining crack depth prior to and during various phases of specimen testing. The method used and the results achieved are described in Appendix A.

2.5 Testing

Table 1 shows the distribution of test specimens among the various types of tests. The test variables included specimen type (4-inch wide weld land, 6- and 12-inch wide uniform thickness, and uncracked tensile), processing (virgin and repair welds, proof stress, and cure time), test temperature ($+70^{\circ}\text{F}$ and -320°F), flaw size and shape and loading procedure (eccentric or symmetrical; static or cyclic).

TABLE 1

TEST PROGRAM

Specimen Type	Weld Thickness (in.)	Weld Type	Processing Sequence	Test Temp. (°F)	Test Loading		
					Static		Cyclic Symmetric
					Symmetric	Eccentric	
Weld Land (Precracked) (Fig. 3)	0.220	Virgin	Not Proof Tested	70	(Specimen numbers shown)		
				-320		1-2, 2-3, 2-2, 3-3	
			Proof Tested	70		7-5	
				-320	6-2, 6-3, 6-6	6-4, 6-5 7-1, 7-3, 7-4 7-6	
6-Inch Wide Uniform Thickness (Fig. 4)	0.191	Virgin	Not Proof Tested	70	V12-1, V12-4, V13-1, V14-2, V15-1, V15-3, V16-4		
				-320	V12-2, V12-3, V14-4		
			Proof Tested and Cured	-320	V13-2, V13-3, V13-4, V14-1,		V14-3, V16-3
				Proof Tested Only	-320	V16-5	
		Repair	Not Proof Tested	70	R8-1, R8-3 R9-2, R10-3, R11-1, R11-2		
				-320	R8-2, R8-4, R9-1, R10-2, R10-4		
			Proof Tested and Cured	-320	R9-3, R9-4, R10-1		R11-4
				Proof Tested Only	70		
			-320	R20-5		R20-2, R20-3 R21-3	

TABLE 1 (Continued)

Specimen Type	Weld Thickness (in.)	Weld Type	Processing Sequence	Test Temp. (°F)	Test Loading All Static Symmetric
12-Inch Wide Uniform Thickness (Fig. 5)	0.191	Virgin	Not Proof Tested	70	V17-1, V17-2 (Surface cracked) V18-1, V18-2 (Through-cracked)
Uncracked Tensile (3/4 Inch Wide Strips)	0.220	Virgin	Not Proof Tested	70	6-7-1, 6-7-2, 6-7-3, 6-7-4, 6-7-5
Uncracked Tensile (Fig. 6)	0.191	Virgin	Not Proof Tested	70	V12-T1, V12-T2, V12-T3 V13-T1, V14-T1, V15-T1
			Proof Tested	-320	V15-4-1, V15-4-2
			Not Proof Tested	70	R8-T1, R8-T2, R8-T3 R9-T1, R10-T1, R11-T1
		Repair	Proof Tested	-320	R21-5-1, R21-5-2

A total of 78 specimens were tested, distributed as follows:

Weld land: 16

Uniform thickness:

Six-inch wide

static 30

cyclic 7

Twelve-inch wide

static 4

Uncracked tensile: 21

TOTAL 78

All tests at 70°F were conducted in ambient laboratory air. All tests at -320°F were conducted with the specimen and grips immersed in liquid nitrogen in a cryostat. Static tests were performed at a loading rate of approximately 5,000 pounds per minute for 4- and 6-inch wide specimens and 10,000 pounds per minute for 12-inch wide specimens. During proof tests and cyclic tests maximum load was maintained for approximately 15 seconds before unloading.

Tensile tests of uncracked specimens employed strain gages bonded to the weld center to provide weld metal yield strength (F_{ty}) and elastic modulus (E_t) data. In addition, conventional 2-inch extensometers were used to provide weld joint yield strength data for comparison.

Methods for eccentric and symmetric loading of weld land specimens, shown in Figure 7, are designed to simulate common types of bending loads which are imposed on the aft dome meridian welds during proof testing and flight conditions.

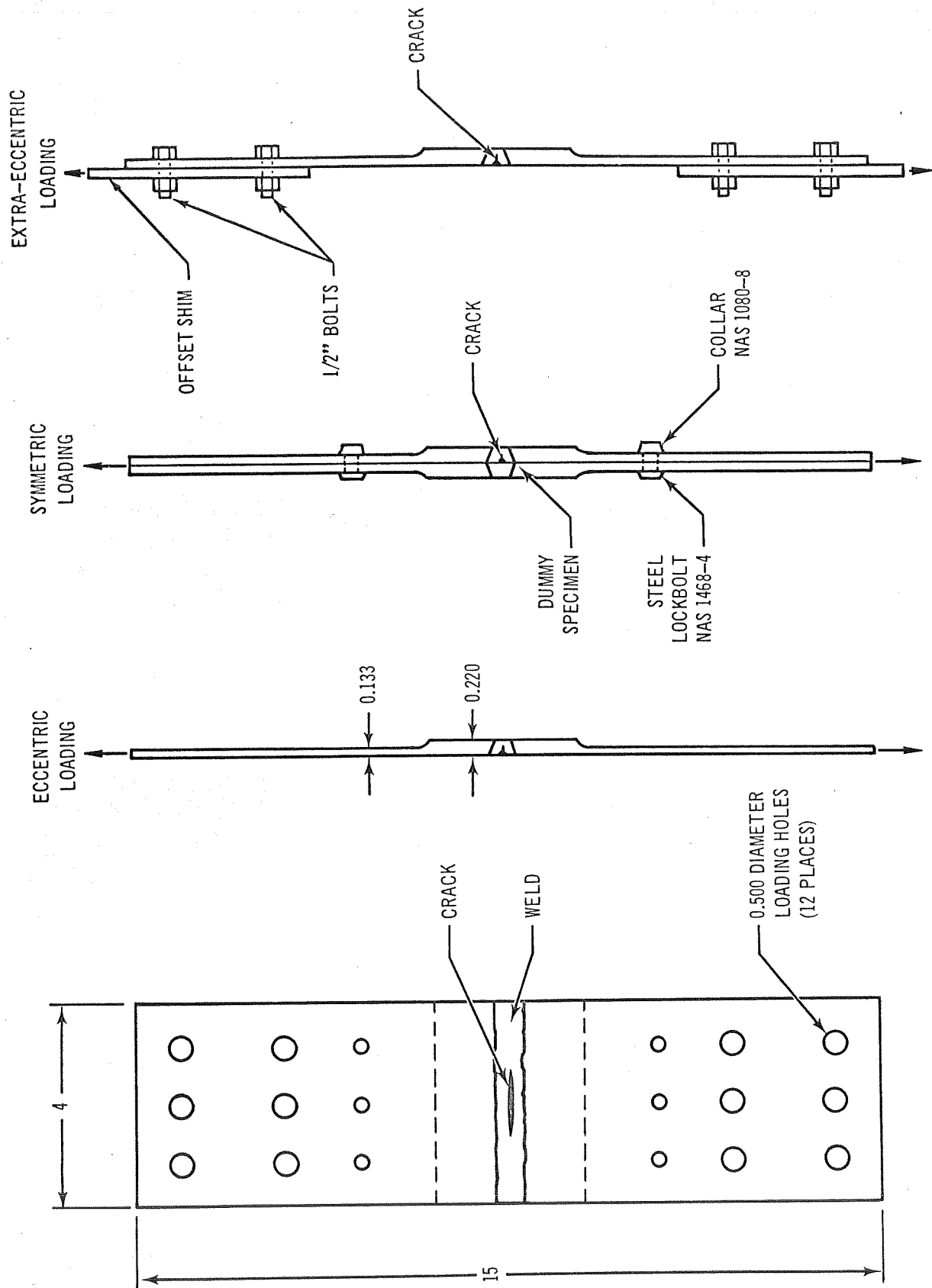


Figure 7. Eccentric and Symmetric Loading

2.6 Data Computation

2.6.1 Partial-Thickness Crack Tests

The results of fracture toughness tests of partial-thickness crack specimens were treated by plotting stress at fracture versus initial flaw size. In order to extend the data bands somewhat beyond the actual test conditions, apparent values of the critical stress intensity, K_{Ic} , were calculated and used in generating data curves. The specimen and crack dimensions, as well as the stresses at fracture, rarely complied with empirical rules established some years ago (References 1, 2) for partial-thickness crack specimen tests. For example, one of these rules states that in order to employ the test results to calculate a valid K_{Ic} the gross stress, σ_g , must be less than the yield strength, σ_y . Maximum operating stress (25.2 ksi) in the LOX dome meridian welds, however, can exceed the yield strength of repaired welds (23.6 ksi) in 2014-T6. To simulate stress levels and crack sizes which may occur in a meridian weld therefore, this rule, as well as certain others, was not invoked. As a result, the calculated apparent values of K_{Ic} for the tests conducted here may not be useful in describing conditions much beyond the bounds of these test conditions. The values are quite useful, however, in comparing the effects of temperature, prior proof loading, and repair welding on the fracture strength of the cracked panels.

The stress value used in the plots of fracture stress versus initial flaw size is the net stress, σ_{nf} , calculated as:

$$\sigma_n = \frac{P}{A_n} = \frac{P}{WB - A_c} \quad [1]$$

where P = fracture load
 A_n = net area
 W = panel width
 B = panel thickness
 A_c = area of crack

In a specimen of finite width, W , the net stress always exceeds the gross stress, σ_g , defined as:

$$\sigma_g = \frac{P}{WB} \quad [2]$$

Figure 8 illustrates the effect of specimen width on the net and gross stresses of a panel of a given thickness containing a crack of a given area. At great panel widths, the net and gross stress both approach a common value (at infinite panel width, gross stress is equal to net stress). The common value which both approach at great widths corresponds to the stress, σ , in a large structure which contains a crack. At small panel widths, both the net and gross stresses are less than σ , but gross stress is the least. Figure 8 illustrates that, for tests of narrow panels containing cracks of relatively large area, use of gross stress leads to a greater underestimate of panel strength than does use of the net stress. Tests of panels of two different widths (6-inches and 12-inches), but containing similar size cracks, were performed to demonstrate the width effect and confirmed the use of net stress for evaluation of narrow (6-inch wide) panels.

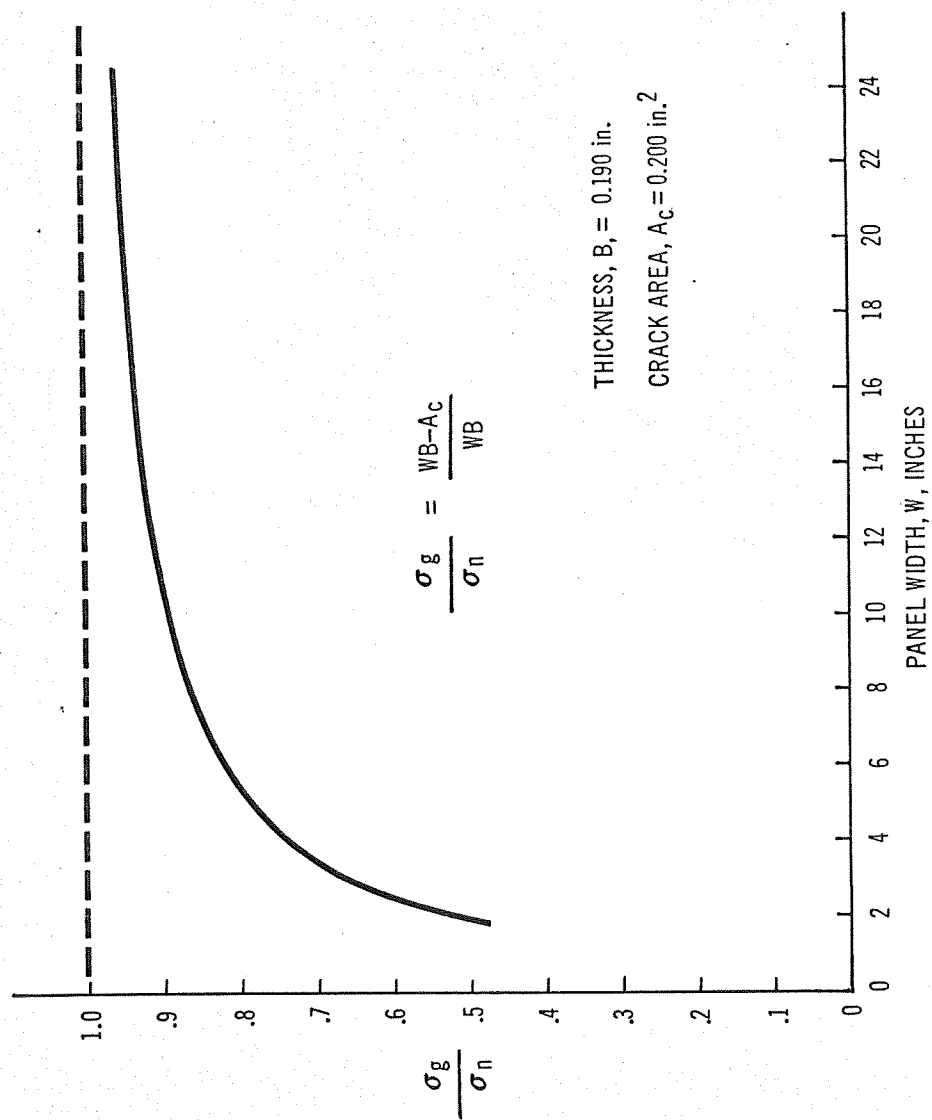


Figure 8. Effect of Width on Ratio of Gross Stress to Net Stress in a Cracked Panel

The use of net stress in describing the test results requires the establishment of a number of conventions. Since flaw enlargement was often observed on rising load, the area of the crack increased during the loading cycle, the gross area remained the same, and the net area decreased. The convention was established that net fracture stress would be calculated using the area of the crack at the time of fracture, as nearly as that area could be determined; if no enlargement of the flaw could be detected, the net fracture stress would be calculated using the initial area of the crack. Crack areas were calculated from:

$$A_c = \frac{\pi}{4} a(2c) \quad [3]$$

where a = depth of partial-thickness crack

$2c$ = surface length of partial-thickness crack

In some tests, the enlargement of the partial crack was so great that prior to fracture the crack extended entirely through the thickness of the specimen. The shape of the crack after extending through the specimen was such that for these cracks the crack area was calculated from:

$$A_c = 1.2 \frac{\pi}{4} B (2c) \quad [4]$$

where B = specimen thickness

$2c$ = surface length of crack (on originally cracked surface)

1.2 = a factor accounting for non-elliptical shape of through-crack

Flaw sizes, a/Q_{nf} , were calculated using net stress from:

$$\frac{a}{Q_{nf}} = \frac{a}{\phi^2 - .212 (\sigma_n/\sigma_y)^2} \quad [5]$$

a = crack depth

σ_n = net stress

σ_y = yield strength

$\phi = 1 + 4.5934 (a/2c)^{1.6499}$

$2c$ = crack length

Initial flaw size, a_i/Q_{nf} , was defined by initial crack dimension, a_i and $2c_i$, and by the net stress at fracture. Final flaw size (e.g.: flaw enlargement due to proof loading) was calculated using equation [5] and the enlarged flaw dimensions.

K_{Ic} values were calculated using initial flaw sizes and both the net stress and gross stress. For net stress, the equation used was:

$$K_{Ic}(\text{net}) = 1.1 \sqrt{\pi} \sigma_{nf} \left(a_i/Q_{nf} \right)^{1/2} \quad [6]$$

where σ_{nf} = net stress at fracture

a_i = initial crack depth

$Q_{nf} = \phi^2 - .212 (\sigma_{nf}/\sigma_y)^2$

For gross stress, the equation used was:

$$K_{Icg} = 1.1 \sqrt{\pi} \sigma_{gf} \left(a_i/Q_{gf} \right)^{1/2} \quad [7]$$

where σ_{gf} = gross stress at fracture

a_i = initial crack depth

$Q_{gf} = \phi^2 - .212 (\sigma_{gf}/\sigma_y)^2$

2.6.2 Through-Thickness Crack Tests

The results of tests on through-cracked, 12-inch wide specimens were treated by plotting gross fracture stress, σ_{gf} , versus length of through-crack at maximum load, ℓ_c . Data bands were extended beyond the test conditions by use of K_c values calculated by:

$$K_c = \sigma_{gf} \sqrt{W \tan \left(\frac{\pi \ell_c}{2W} \right)} \quad [8]$$

where σ_{gf} = gross fracture stress

W = specimen width

ℓ_c = length of crack at failure (critical length)

Values of nominal stress intensity, K_{CN} , were also calculated with equation [8] but using initial crack length, ℓ_o , instead of the critical length, ℓ_c . Because of geometric and mathematic limitations, the values of K_c could not be corrected for plastic strain and the reported values are therefore low.

3.0 RESULTS

3.1 Weld Land Specimens

Weld land specimens with 5:3 reinforcement were tested to determine the effect of bending stresses on the strength of surface-cracked welded panels. In addition to static fracture tests of 4-inch wide precracked specimens, two specimens were instrumented with strain gages to obtain bending data, and five 3/4-inch wide strip tensile specimens were tested to obtain the uniaxial tensile properties of the weld.

3.1.1 Tensile Properties of Weld Lands

Room temperature uniaxial tensile properties of transverse weld specimens cut from the weld land of specimen 6-7 are listed in Table 2. The average properties ($F_{ty} = 22.8$ ksi, $F_{tu} = 44.1$ ksi, $E_t = 11,700,000$ psi) were used to evaluate the results of the bending and fracture tests described below, and to characterize the weld land material. All welds were shaved and all specimens failed in the weld.

3.1.2 Bending in Weld Lands

In order to determine the magnitude of bending caused by eccentric loading of partial-thickness crack weld land specimens, two 4-inch wide specimens were used. (By mistake, excessively long EDM notches, 2-inches long, had been placed in these specimens. The influence of surface flaws upon the nature of bending was, therefore, accentuated in these tests).

Strain gages were cemented to the specimens as shown in Figures 9 and 10 on both X (exterior) and Z (interior) faces in two locations. One pair of strain gages (shown as triangular symbols) was located on the weld centerline, one-half inch from the edge of the specimen. The other pair of strain gages (shown as circular symbols) was centered on the parent metal of the weld land, one-half inch from the weld centerline. The strains listed in Table 3 were obtained by incremental loading to the gross stresses listed in the same table. The strain ratios, which are direct measures of the extent of bending due to eccentric loading, are listed in Table 3 and plotted versus gross stress in Figures 9 and 10.

TABLE 2

RESULTS OF WELD LAND TENSILE TESTS

Specimen Number	Weld Type	Width (in.)	Thick. at Weld (in.)	Temp. ($^{\circ}$ F)	Weld F_{ty} (ksi)	Weld F_{tu} (ksi)	Weld E_t (10^6 psi)	Failure Location
6-7-1	Virgin	.730	.226	70	----	43.9	----	Weld
6-7-2		.737	.223		----	43.6	----	Weld
6-7-3		.722	.224		----	43.3	----	Weld
6-7-4		.766	.207		22.9	44.6	11.7	Weld
6-7-5		.780	.209		22.6	45.3	11.7	Weld
Average					<u>22.8</u>	<u>44.1</u>	<u>11.7</u>	

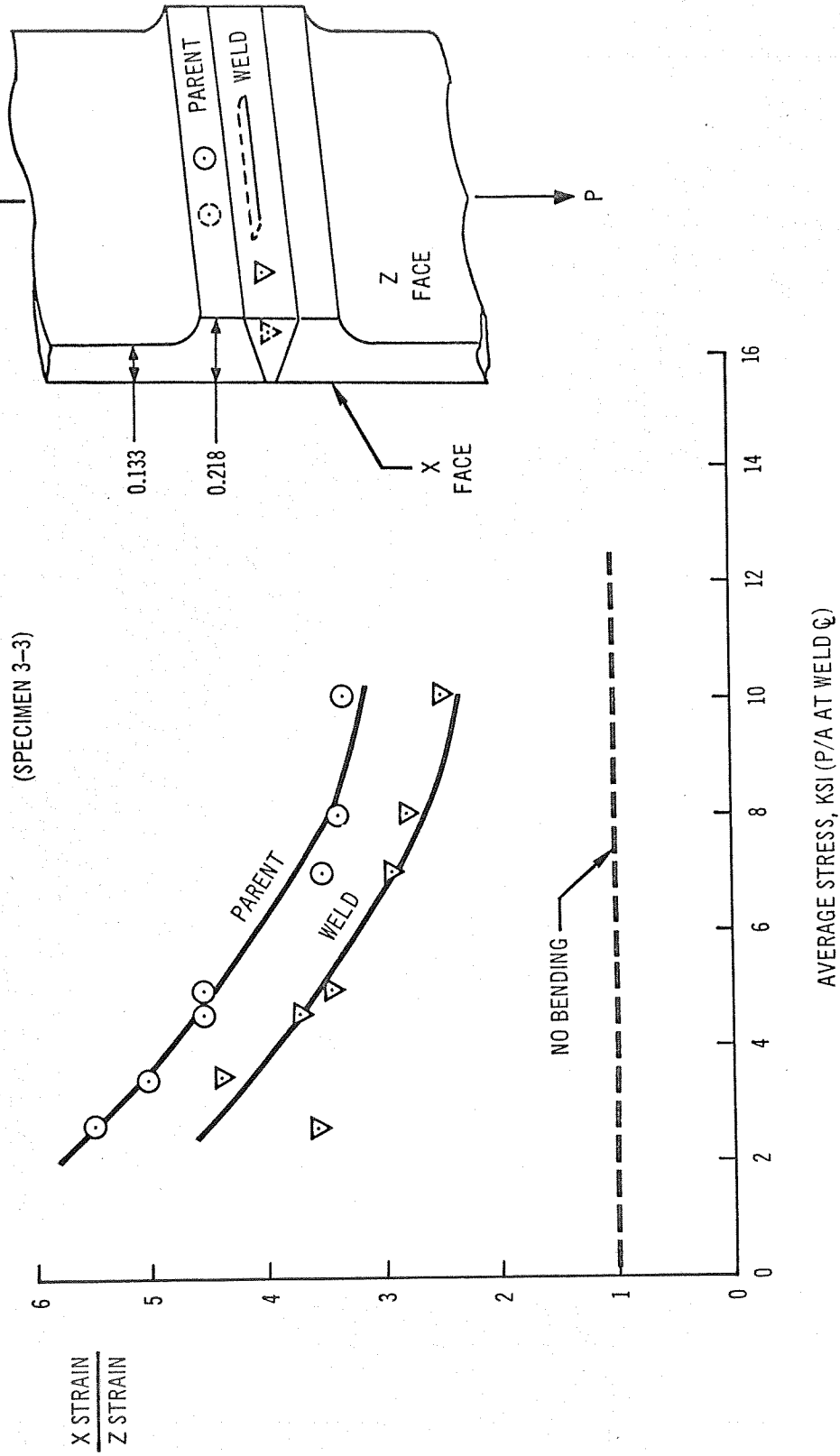


Figure 9. Bending in 5:3 Weld Land with Interior Surface Notch

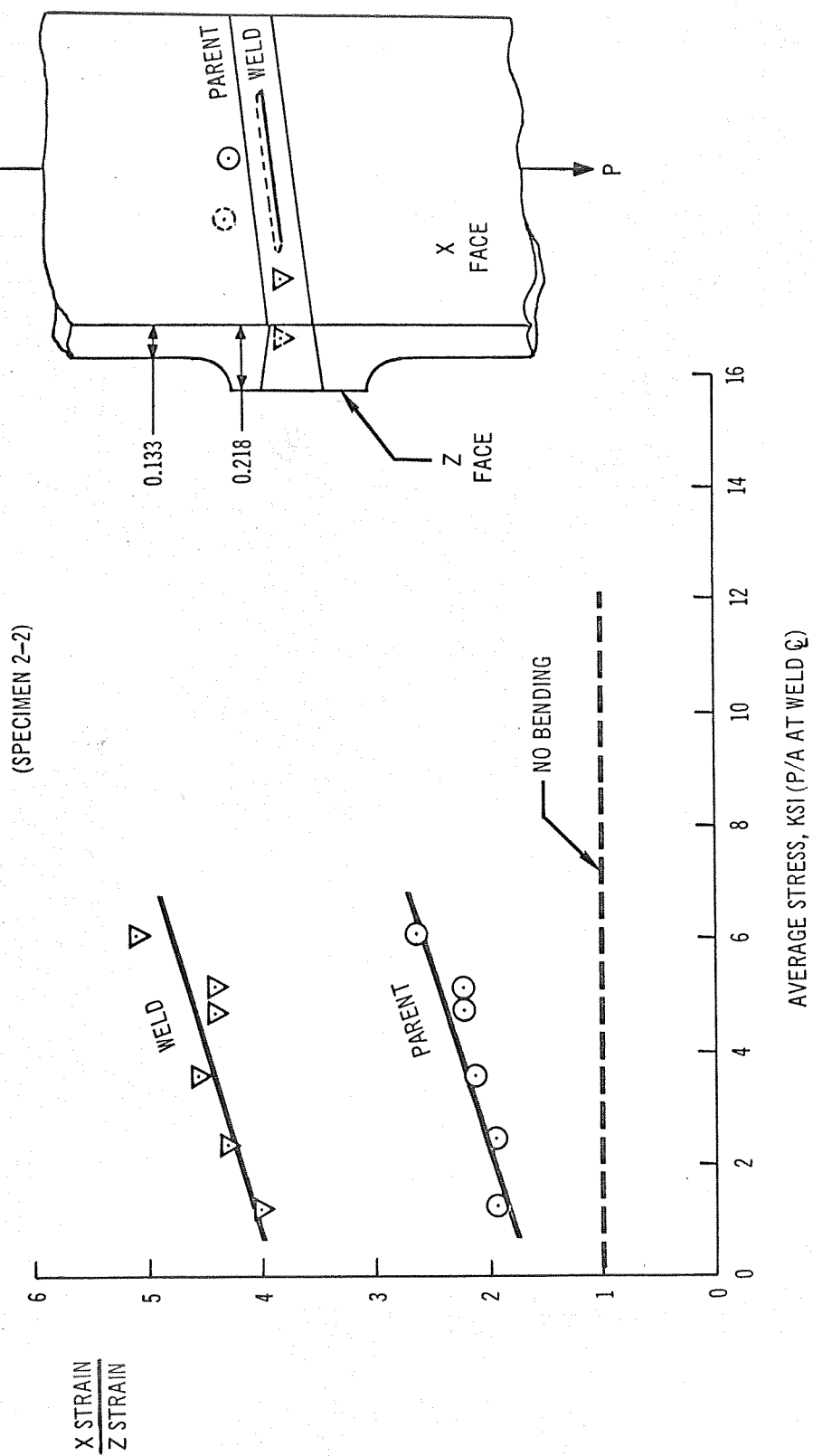


Figure 10. Bending in 5:3 Weld Land with Exterior Surface Notch

TABLE 3

WELD LAND STRAIN GAGE DATA

Specimen Number	Gross Stress σ_g (psi)	Strain, ϵ , (10^{-5} inches)				Strain Ratio $\epsilon_x : \epsilon_z$	
		Weld		Parent		Weld	Parent
		X Face	Z Face	X Face	Z Face		
<u>3-3</u>	2310	18	5	22	4	3.6	5.5
Notch on Interior (Z) Face	3470	40	9	40	8	4.4	5.0
	4620	52	14	58	13	3.7	4.5
	5000	55	16	63	14	3.4	4.5
	7000	88	30	98	28	2.9	3.5
	8000	115	41	122	36	2.8	3.4
	10,000	150	59	150	46	2.5	3.3
<u>2-2</u>	1150	8	2	8	4	4.0	1.9
Notch on Exterior (X) Face	2300	26	6	22	11	4.3	1.9
	3450	43	10	36	17	4.5	2.1
	4600	60	14	51	23	4.4	2.2
	5000	65	15	55	25	4.4	2.2
	6000	79	16	66	26	5.1	2.5

The curves indicate that, for interior notches, bending is rather severe at very low stresses but falls off rapidly as stress is increased. Exterior surface notches apparently result in accentuated bending which increases as the stress is increased in the low stress range. No data was obtained on bending at high stress levels (above 10 ksi gross stress).

3.1.3 Static Fracture Tests of Weld Lands

Results of fracture tests of weld land specimens at 70°F and -320°F are listed in Table 4. All specimens contained partial-thickness cracks on the exterior (X) face, with the exception of specimen 3-3, which contained a notch on the interior (Z) face.

Simple tensile loading of weld land panels by gripping the chem-milled region causes eccentric loading of the weld, as shown in Figure 7, which results in higher stresses on the exterior (X) face than on the interior (Z) face. Eccentric proof-loading of weld land specimens caused considerable flaw growth in all specimens except 6-1, which had the smallest initial flaw size of all the specimens tested. The fracture surfaces of specimens 7-4 and 7-1 (shown in Figures 11 and 12, respectively) clearly exhibited the crack growth which occurred during eccentric proof testing at 70°F. Extra-eccentric loading, described in Figure 7, of specimen 6-5 caused the precrack to penetrate the thickness of the weld during the proof test, as shown in Figure 13. Symmetric proof loading of "back-to-back" weld land specimens caused a small amount of crack growth in specimen 7-3 and no observable growth in the rest of the specimens. The fracture

TABLE 4

WELD LAND STATIC FRACTURE TOUGHNESS TEST RESULTS

SPECIMEN			INITIAL FLAW SIZE				PROOF TEST		FLAW SIZE AFTER PROOF				STATIC FRACTURE TEST					NOTES							
Specimen Number	Weld Type	Width, W (in.)	Thickness at Weld, B (in.)	Depth, a_1 (in.)	Length, $2c_1$ (in.)	Shape, $a_1/2c_1$	Size, a_1/a_{nf} (in.)	Loading Type*	Proof Test Temperature ($^{\circ}$ F)	Gross Stress σ_{gp} (ksi)	Net Stress σ_{np} (ksi)	Depth, a_p (in.)	Length, $2c_p$ (in.)	Shape, $a_p/2c_p$	Size, a_p/a_{nf} (in.)	Loading Type*	Test Temperature	Weld Fty (ksi)	Gross Stress, σ_{gt} (ksi)	Net Stress, σ_{nt} (ksi)	Apparent*** K_{Ic}	Apparent*** K_{Ic}	Apparent*** K_{Ic} (net)		
1-2	Virgin	4.003	0.229	0.155	1.156	0.134	0.162		Not proof tested								E	70	22.8	21.0	24.8	16.2	19.5		
2-3	Virgin	4.002	0.227	0.153	1.140	0.134	0.160		Not proof tested								E	70	22.8	21.0	24.7	16.1	19.3		
6-4**	Virgin	4.000	0.225	0.085	0.336	0.252	0.067	S	70	19.2	19.7		No growth				-	70	----	----	----	----	----		
				0.085	0.336	0.252	0.067	E	-320	31.1	32.4	0.130	0.357	0.364	0.078		E	70	22.8	30.2	31.5	15.3	15.9		Unusual history
2-2	Virgin	4.002	0.225	Thru	2.160	0.104	----		Not proof tested								E	70	22.8	12.5	25.4	----	----		Crack too long; invalid.
3-3****	Virgin	4.000	0.226	0.173	2.156	0.080	----		Not proof tested								E	70	22.8	13.6	20.1	----	----		Crack too long; invalid.
7-5	Virgin	3.998	0.229	0.136	1.107	0.122	0.134		Not proof tested								E	-320	30.0	20.5	23.5	14.4	16.8		Doubtful
6-1	Virgin	4.001	0.226	0.080	0.337	0.237	0.065	E	70	19.2	19.7						E	-320	30.0	35.2	36.0	17.6	18.0		
7-1	Virgin	3.998	0.229	0.145	1.106	0.131	0.143	E	70	19.2	23.6	0.190	1.154	0.164	0.179		E	-320	30.0	22.0	27.1	16.0	20.0		
7-4	Virgin	4.000	0.229	0.140	1.081	0.129	0.138	E	70	19.2	22.9	0.174	1.093	0.159	0.163		E	-320	30.0	21.5	25.7	15.3	18.6		
7-6	Virgin	3.996	0.229	0.150	1.092	0.137	0.145	S	70	19.2	22.3		No growth				E	-320	30.0	21.0	24.4	15.3	18.2		
7-3	Virgin	4.000	0.228	0.147	1.115	0.131	0.145	S	70	19.2	22.5	0.153	1.115	0.137	0.150		E	-320	30.0	22.0	25.8	16.1	19.2		
6-3	Virgin	3.990	0.225	0.083	0.328	0.253	0.065	S	70	19.2	19.7		No growth				S	-320	30.0	37.4	38.3	18.7	19.1		
6-2	Virgin	4.004	0.225	0.147	1.106	0.132	0.154	S	70	19.2	22.4		No growth				S	-320	30.0	26.8	31.2	20.1	23.9		
6-6	Virgin	3.996	0.226	0.146	1.108	0.131	0.145	E	70	19.2	23.8	0.193	1.154	0.167	0.181		S	-320	30.0	22.1	27.4	16.1	20.4		
6-5	Virgin	3.997	0.225	0.147	1.102	0.133	0.147	XE	70	19.2	26.7	Thru	1.194	0.188	0.208		E	-320	30.0	22.8	31.7	16.7	23.7		

Nominal weld land thickness = 0.220 in.; nominal membrane thickness = 0.133 in. (5:3 reinforcement)

* E = eccentric; S = symmetric (back-to-back); XE = extra-eccentric (offset shims). See Figure 7.

** Proof tested twice (in order listed).

*** Due to bending stresses, continuous growth of the cracks occurred. Thus, the net stress applied was continuously increasing above the value of σ_{nf} given. The resulting "apparent K_{Ic} " values are therefore less than true K_{Ic} values because σ_{nf} was less than the true net stress at fracture by some undetermined amount.

**** Crack located on Z face in this specimen only.

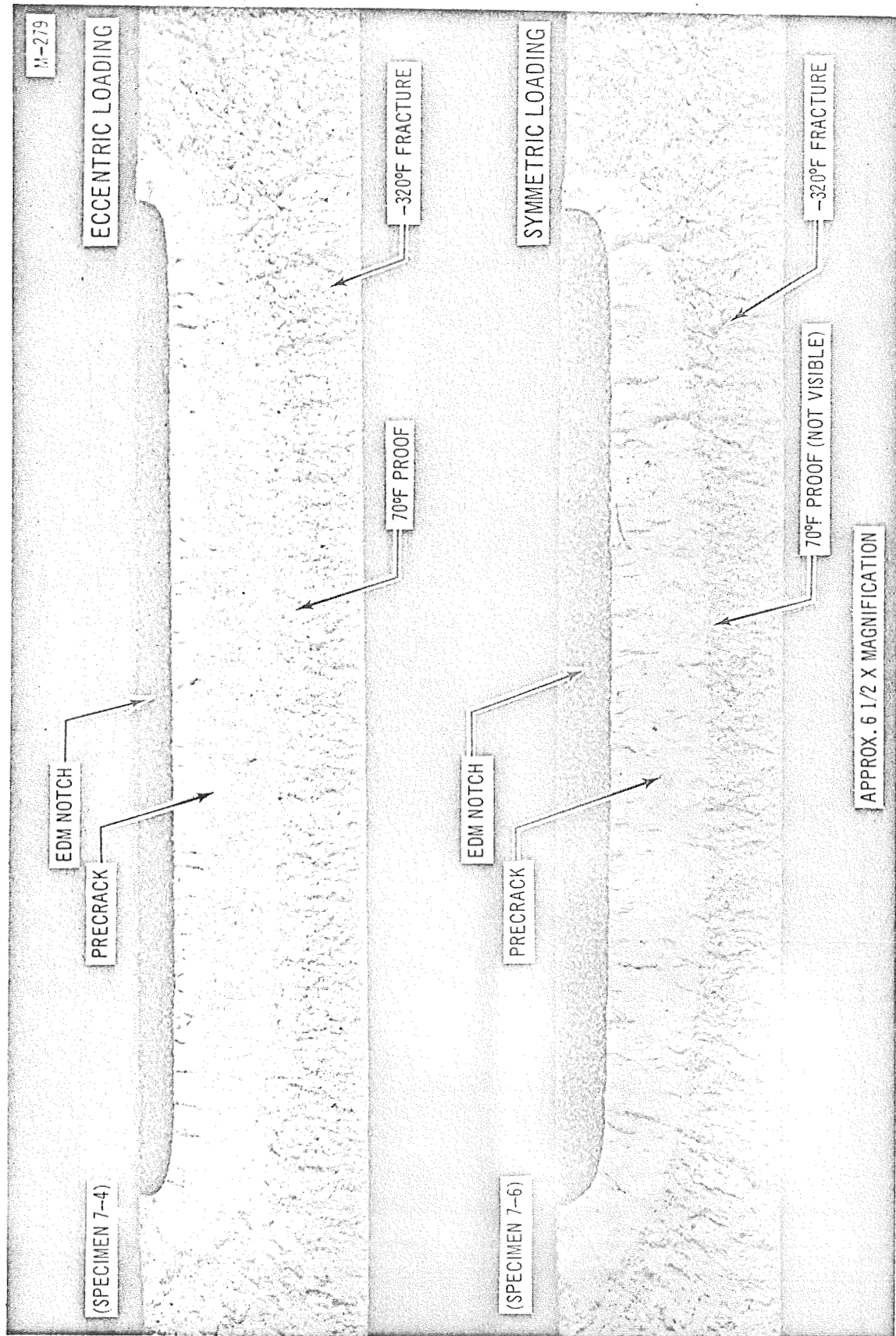


Figure 11. Flaw Growth Due to Bending During 70°F Proof Test of Specimens 7-4 and 7-6

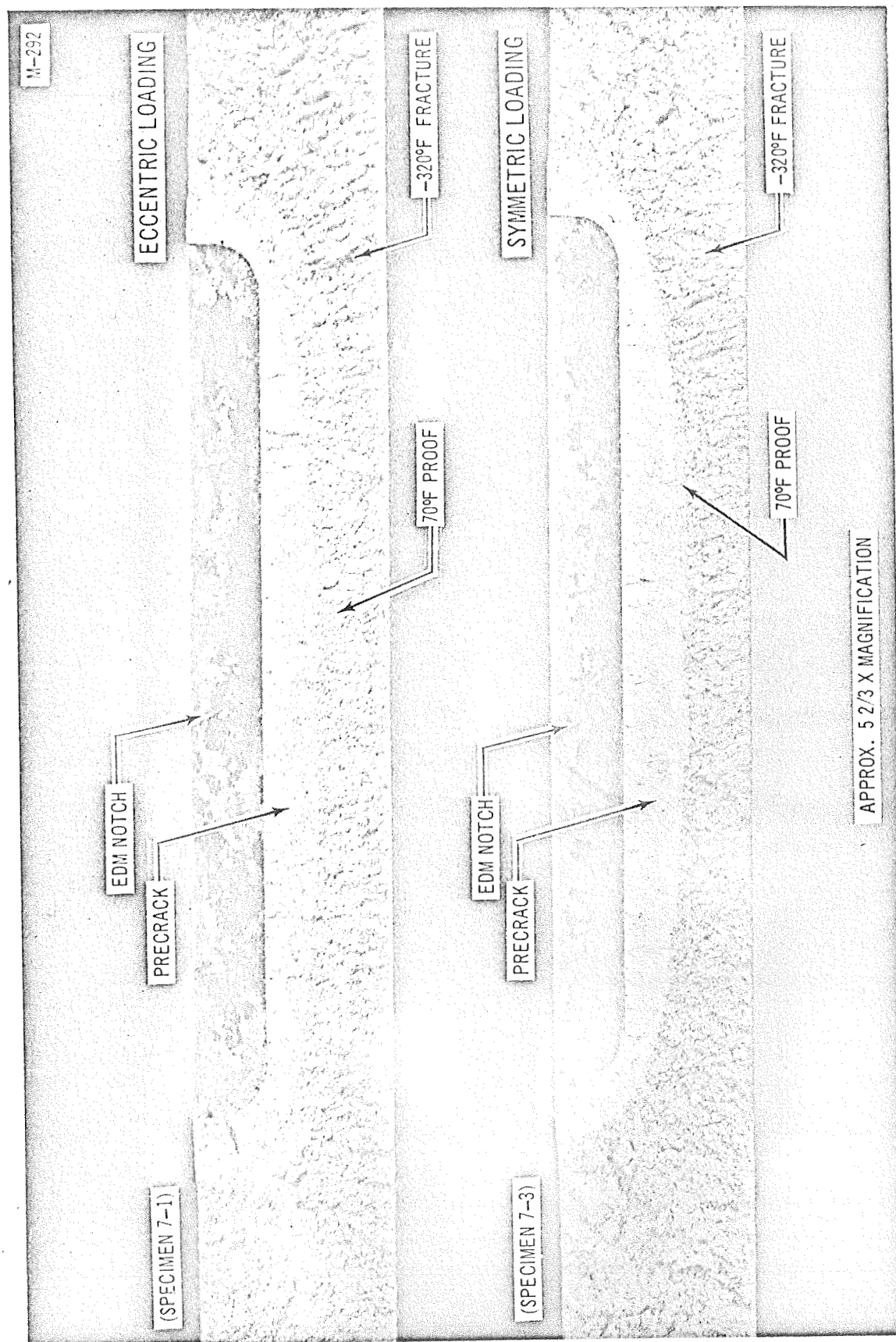


Figure 12. Flaw Growth Due to Bending During 70°F Proof Test of Specimens 7-1 and 7-3

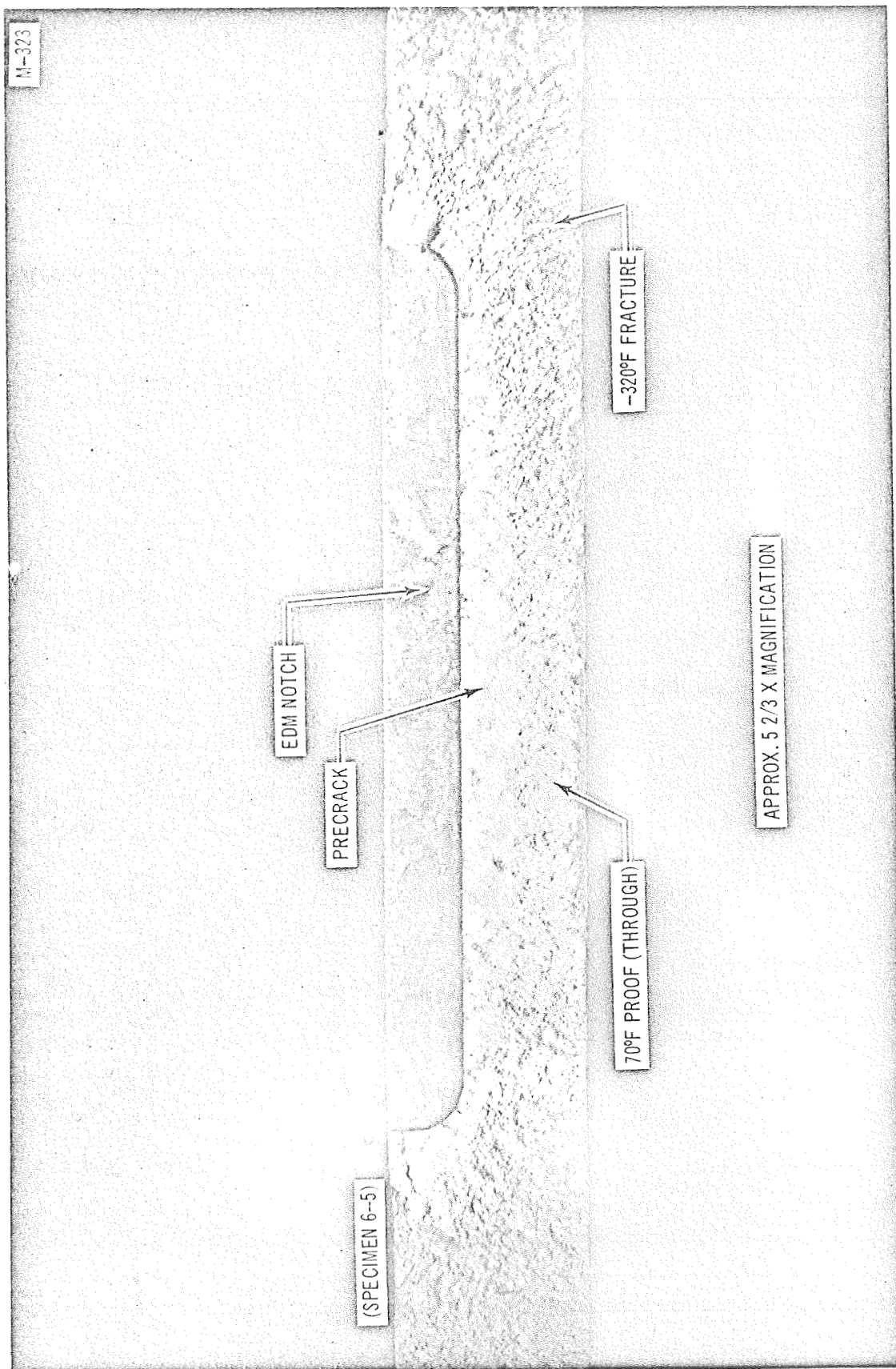


Figure 13. Flaw Growth Due to Extra-Eccentric Proof Test at 70°F

surfaces of specimen 7-6 (Figure 11) exhibited no visible flaw growth, and the fracture surface of specimens 7-3 (Figure 12) exhibited only a small amount of flaw growth due to the proof loading. It should be recalled that the presence of the flaw itself causes some bending in the weld. In addition, the "back-to-back" configuration minimizes the eccentricity of loading, but probably does not eliminate it. Figure 14 summarizes the flaw growth data of Table 4 and demonstrates that flaw growth during proof testing at 70°F is increased by increased eccentricity of loading and by increased initial flaw size.

3.2 Uniform Thickness Specimens

3.2.1 Tensile Properties of Meridian Welds

Uniaxial tensile properties were determined for the uniform thickness welds at 70°F and at -320°F to provide yield strength values for K_{Ic} calculations. The specimens were tested using strain gages on the weld deposit as well as with a 2-inch extensometer to determine yield values by two different methods. The strain gages provided yield values for the weld deposit only. Since the fracture toughness specimens failed in the pre-cracked weld deposit, these weldmetal values were used in the fracture toughness calculations. Uniaxial tensile properties for uniform thickness weldments are listed in Table 5. To provide yield strength data for welds proof tested at 70°F and then tested at -320°F, two virgin and two repair weld tensile specimens were proof tested at 70°F and then tensile tested at -320°F. The results of these tests are listed in Table 6, and were used to calculate flaw sizes and stress intensities in proof tested uniform thickness precracked specimens.

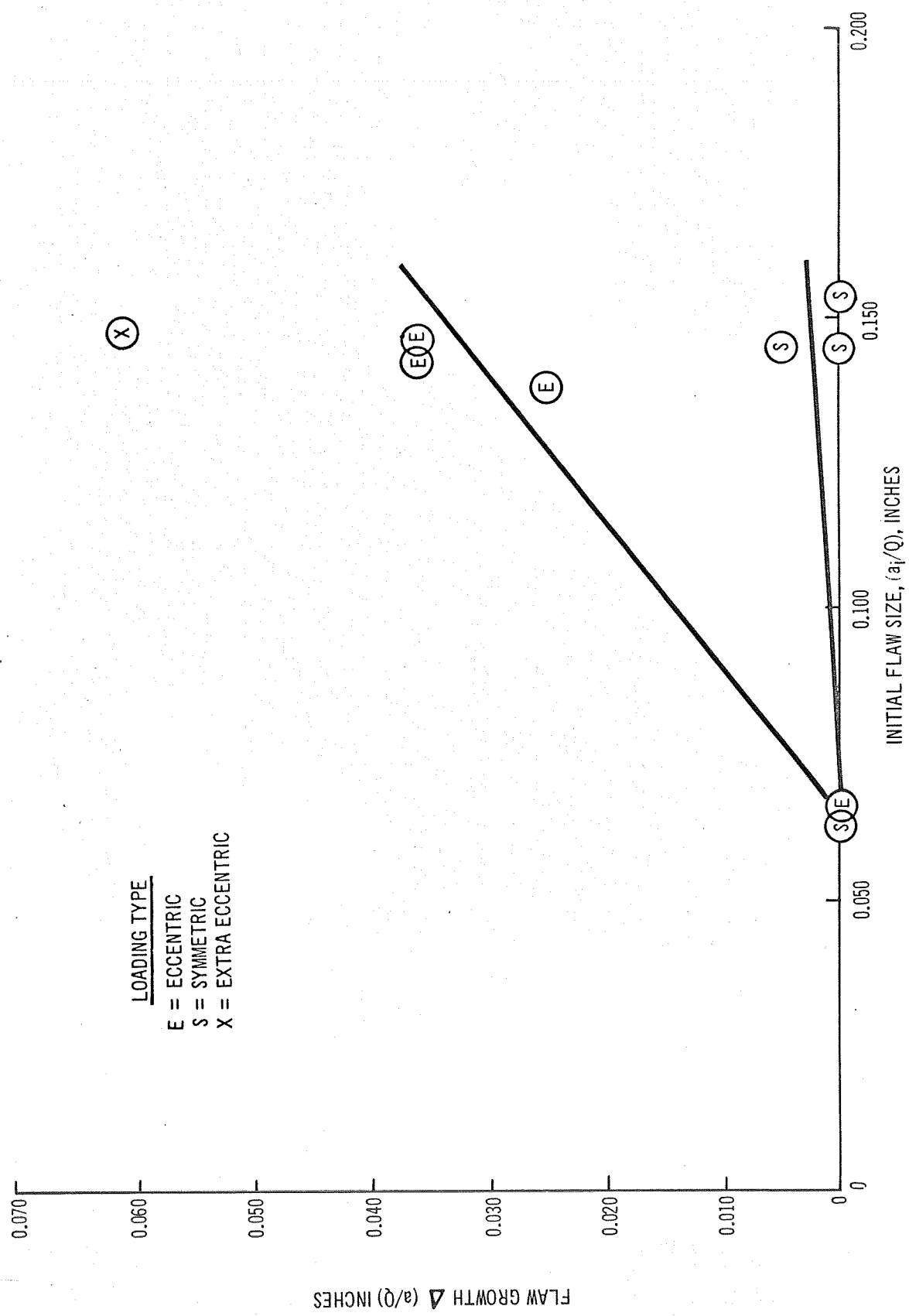


Figure 14. Flaw Growth in Weld Lands During Eccentric and Symmetric Proof Testing

TABLE 5

TENSILE PROPERTIES OF UNIFORM THICKNESS WELDS AT 70°F AND -320°F

Specimen Number	Weld Type	Width (in.)	Thick. at Weld (in.)	Temp. (°F)	Joint F _{ty} (ksi)	Weld F _{ty} (ksi)	Weld F _{tu} (ksi)	Weld E _t (10 ⁶ psi)	Elong. in 1/2" (%)	Elong. in 1" (%)	Elong. in 2" (%)	Failure Location
V12-T1	Virgin	.501	.1915	70	26.6	22.0	44.4	10.4	12	7	4	Weld
V12-T2	Virgin	.502	.1915	70	26.0	22.4**	41.6	9.8**	12	7	4	Weld
V12-T3	Virgin	.502	.1914	70	28.1	22.3	42.5	11.1	12	7	4	Weld
Average					26.9	22.2	42.8	10.4	12	7	4	
V13-T1	Virgin	.500	.1908	-320	36.2	28.5	50.8	11.5	10	5	2	Weld
V14-T1	Virgin	.493	.1912	-320	37.3	29.9	50.6	13.6	8	5	2	Weld
V15-T1	Virgin	.503	.1889	-320	36.3	31.6	50.5	11.6	8	4	2	Weld
Average					36.6	30.0	50.6	12.2	9	5	2	
R8-T1	Repair	.503	.1918	70	22.8	18.5*	36.9	10.5**	8	7	3	Weld
R8-T2	Repair	.502	.1914	70	22.9	19.3	39.1	12.0	12	6	4	Weld
R8-T3	Repair	.499	.1882	70	22.8	17.0*	37.7	6.6*	12	7	4	Weld
Average					22.8	18.7	37.9	11.3	11	7	4	
R9-T1	Repair	.502	.1900	-320	30.5	24.4	47.1	10.2	10	5	2	Weld
R10-T1	Repair	.504	.1889	-320	31.4	22.9	46.9	12.1	10	4	3	Weld
R11-T1	Repair	.503	.1930	-320	----	23.5	45.2	10.0	10	4	2	Weld
Average					31.0	23.6	46.4	10.8	10	4	2	

* Not included in average due to excessive weld peaking which caused bending of specimen.

** Average of strain gage data for torch and root sides of weld. Other F_{ty} and E_t data for welds are based on strain gage data for torch side only.

TABLE 6

TENSILE PROPERTIES OF UNIFORM THICKNESS WELDS
AT -320°F AFTER PROOF TESTING AT 70°F

Specimen Number	Weld Type	Width (in.)	Thickness at Weld (in.)	Net Proof Stress (ksi)	Weld F _{ty} (ksi)	Weld F _{tu} (ksi)	Elong. in 1" (%)	Failure Location
V15-4-1	Virgin	.511	.186	22.3	32.2	58.5	3	Weld
V15-4-2	Virgin	.518	.189	22.3	33.0	58.5	3	Weld
Average					32.6	58.5	3	
R21-5-1	Repair	.498	.190	21.0	31.2	48.9	3	Weld
R21-5-2	Repair	.512	.189	21.0	32.4	52.2	3	Weld
Average					31.8	50.6		

3.2.2 Static Fracture Tests of Meridian Welds

Uniform thickness precracked specimens of two widths were tested in this program. Six-inch wide specimens (Figure 5) with artificial partial-thickness cracks in the center of the weld underbead were loaded to fracture at 70°F and -320°F to determine critical stress intensity factors (K_{Ic}), and fracture strengths. In addition, two similarly cracked partial-thickness crack specimens, 12-inches wide, were tested statically at 70°F to evaluate the applicability of net section fracture strength data from the 6-inch wide specimens to large structures such as the S-IVB LOX tank. Also, two through-cracked 12-inch wide specimens were tested statically at 70°F to verify previous data (Reference 3).

Static test results for all 6-inch wide partial-thickness specimens are listed in Table 7. In addition, the results are depicted graphically as net fracture strength versus initial (precrack) flaw size at 70°F in Figure 15, at -320°F after 70°F proof testing in Figure 16 and at -320°F without prior proof testing in Figure 17. In each figure, the maximum and minimum value of K_{Ic} obtained is used to establish the scatter band for the data. Values of flaw shape, net stress and K_{Ic} were calculated according to equations [1] through [7] above.

During 70°F proof testing, flaw growth occurred and was easily measured on the fracture surfaces, as shown in Figure 18. In addition to depth-wise and lengthwise growth, the gap width of the crack was observed to increase, as shown in Figure 19. This phenomenon, described as "gaposis" allows initially fine or "tight" cracks to be easily detected by visual

TABLE 7

STATIC FRACTURE TEST RESULTS FOR UNIFORM THICKNESS PARTIAL-THICKNESS CRACK SPECIMENS

Specimen Number and Type	Width, W (in.)	Thickness at Weld, B, (in.)	INITIAL FLAW SIZE				PROOF TEST			FLAW DIMENSIONS AFTER PROOF TEST		STATIC FRACTURE TEST				K _{IC}		NOTES
			Depth, a ₁ (in.)	Length, 2c ₁ (in.)	Shape, a ₁ /2c ₁	Size, a ₁ /a _{np} (in.)	Proof Test Temp. (°F)	Gross Stress, σ _{gp} (ksi)	Net Stress, σ _{np} (ksi)	Depth, a _p (in.)	Length, 2c _p (in.)	Test Temp. (°F)	Weld F _{ty} (ksi)	Gross Stress, σ _{gt} (ksi)	Net Stress, σ _{nt} (ksi)	Apparent K _{ICg} (ksi√in)	Apparent K _{ICnet} (ksi√in)	
V12-1	6.016	0.192	0.148	1.296	0.114	0.161	Not Proof Tested	Proof Tested	---	---	70	22.2	22.9	26.3	17.9	20.6	Popped thru at σ _g = 21.6 ksi	
V12-4	6.016	0.192	0.152	1.496	0.101	0.170	Not Proof Tested	Proof Tested	---	---	70	22.2	21.5	25.4	17.2	20.5		
V13-1	6.002	0.192	0.127	1.087	0.116	0.137	Not Proof Tested	Proof Tested	---	---	70	22.2	23.5	25.9	17.0	18.8		
V14-2	6.014	0.191	0.126	0.712	0.176	0.119	Not Proof Tested	Proof Tested	---	---	70	22.2	29.5	31.4	19.9	21.2		
V15-1	6.010	0.188	0.145	1.964	0.073	0.170	Not Proof Tested	Proof Tested	---	---	70	22.2	21.3	26.6	17.0	21.4	Insufficient precrack extension from EDM notch; not included in average.	
V15-3	6.008	0.189	Thru	2.090	----	----	Not Proof Tested	Proof Tested	---	---	70	22.2	20.2	30.1	----	----		
V16-4	6.009	0.193	0.147	1.067	0.137	0.152	Not Proof Tested	Proof Tested	---	---	70	22.2	25.6	30.7	19.5	23.4		
R8-1	6.012	0.193	0.113	1.091	0.103	0.125	Not Proof Tested	Proof Tested	---	---	70	18.7	24.6	26.8	17.0	18.6		
R8-3	6.010	0.192	0.082	1.006	0.081	0.095	Not Proof Tested	Proof Tested	---	---	70	18.7	24.7	26.2	14.9	15.7	Popped thru at σ _g = 23.7 ksi Popped thru at σ _g = 21.5 ksi	
R9-2	6.007	0.186	0.149	1.495	0.099	0.167	Not Proof Tested	Proof Tested	---	---	70	18.7	21.2	25.1	16.9	20.0		
R10-3	5.993	0.190	0.125	0.704	0.177	0.118	Not Proof Tested	Proof Tested	---	---	70	18.7	26.6	28.3	17.9	19.0		
R11-1	6.019	0.192	0.139	1.946	0.071	0.164	Not Proof Tested	Proof Tested	---	---	70	18.7	18.9	23.2	14.9	18.3		
R11-2	6.014	0.194	Thru	2.118	----	----	Not Proof Tested	Proof Tested	---	---	70	18.7	17.5	26.2	----	----	Insufficient precrack extension from EDM notch; not included in average.	
V17-1	12.010	0.191	0.124	1.953	0.063	0.148	Not Proof Tested	Proof Tested	---	---	70	22.2	25.3	29.9	18.9	22.4		
V17-2	12.010	0.190	0.150	1.291	0.116	0.163	Not Proof Tested	Proof Tested	---	---	70	22.2	27.5	30.6	21.7	24.1		
V12-2	5.998	0.194	0.132	1.106	0.119	0.141	Not Proof Tested	Proof Tested	---	---	-320	30.0	26.5	29.4	19.0	21.5		
V12-3	5.999	0.193	0.138	1.294	0.106	0.152	Not Proof Tested	Proof Tested	---	---	-320	30.0	27.7	31.5	20.8	24.0	Cured 64 hours at + 160°F after proof testing.	
V14-4	6.015	0.194	0.145	1.962	0.073	0.158	Not Proof Tested	Proof Tested	---	---	-320	30.0	20.1	24.9	15.2	19.3		
R8-2	6.010	0.192	0.125	1.107	0.112	0.136	Not Proof Tested	Proof Tested	---	---	-320	23.6	24.3	26.8	17.5	19.3		
R8-4	6.010	0.191	0.092	1.008	0.083	0.106	Not Proof Tested	Proof Tested	---	---	-320	23.6	25.3	27.2	16.1	17.3		
R9-1	6.008	0.189	0.153	1.500	0.102	0.170	Not Proof Tested	Proof Tested	---	---	-320	23.6	19.6	23.3	15.3	18.7	Cured 65 to 70 hours at + 160°F after proof testing.	
R10-2	5.992	0.190	0.121	0.704	0.171	0.116	Not Proof Tested	Proof Tested	---	---	-320	23.6	28.2	30.0	18.8	19.9		
R10-4	6.004	0.190	0.132	1.960	0.067	0.156	Not Proof Tested	Proof Tested	---	---	-320	23.6	20.8	25.3	15.6	19.5		
V13-2	6.011	0.192	0.121	1.094	0.110	0.128	70	17.3	19.0	No growth	2.200	-320	32.6	27.5	30.2	21.1		
V13-3	6.013	0.192	0.144	1.300	0.110	0.146	70	16.0	18.6	0.153	1.352	-320	32.6	22.8	26.5	16.7		19.8
V13-4	6.015	0.192	0.146	1.503	0.097	0.154	70	14.7	17.3	No growth	---	-320	32.6	23.6	27.7	17.7	21.3	
V14-1	6.020	0.191	0.148	1.688	0.087	0.156	70	13.8	16.6	No growth	---	-320	32.6	21.9	26.4	16.5	20.4	
V16-5	6.011	0.193	0.167	2.045	0.081	0.177	70	15.4	23.5	Thru	---	-320	32.6	19.8	30.2	----	----	
R9-3	6.005	0.189	0.128	1.101	0.116	0.131	70	17.6	20.1	0.152	1.186	-320	31.8	24.9	28.4	17.4	20.1	
R9-4	6.005	0.188	0.143	1.292	0.110	0.151	70	17.0	19.9	0.158	1.338	-320	31.8	25.5	29.9	18.9	22.7	
R10-1	5.990	0.188	0.154	1.488	0.103	0.158	70	15.7	21.2	Thru	---	-320	31.8	21.6	29.1	----	----	
R20-5	5.987	0.186	0.179	1.967	0.091	0.183	70	16.1	25.2	Thru	2.290	-320	31.8	17.4	27.2	----	----	

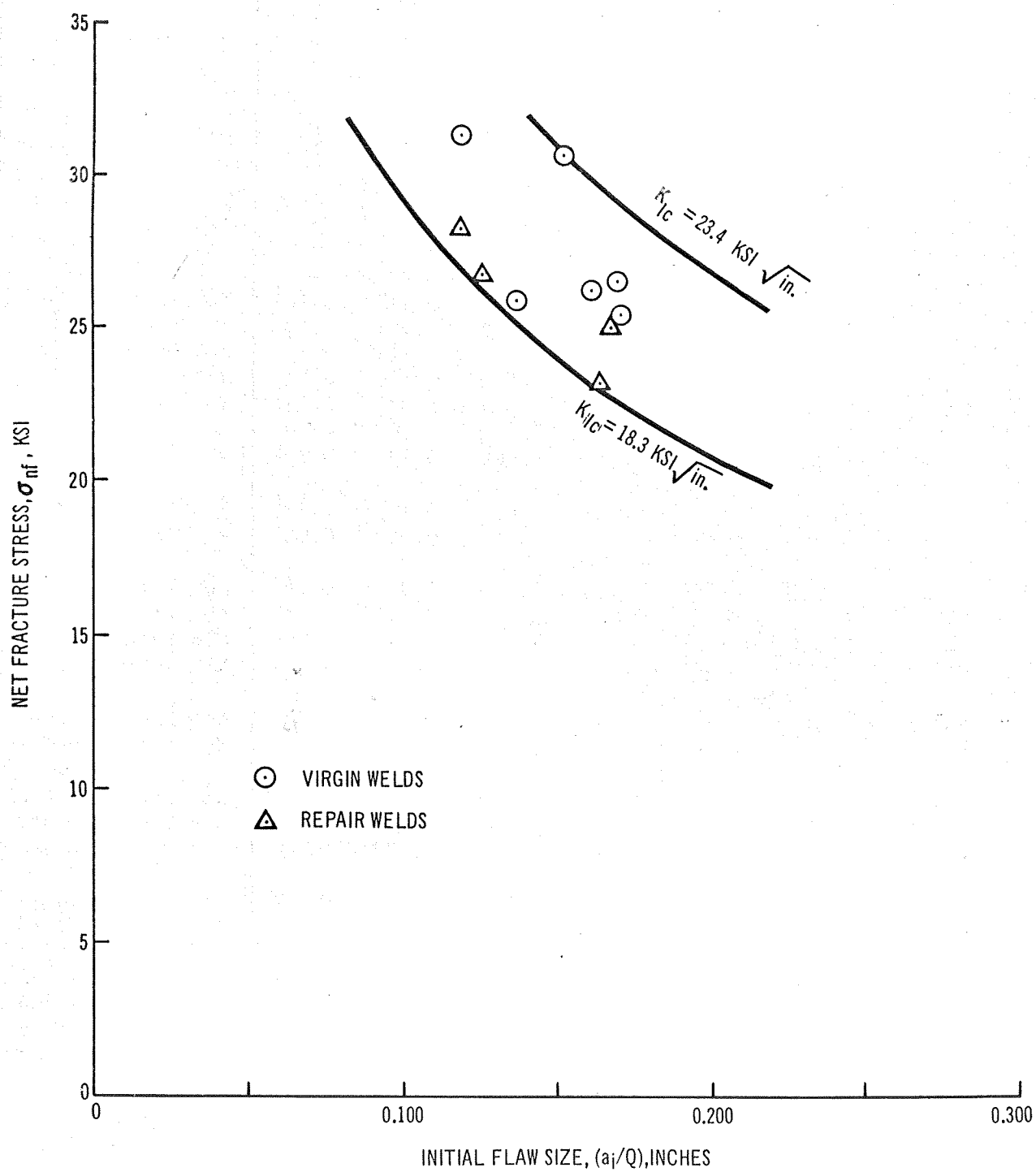


Figure 15. Stress Vs. Flaw Size for Partial-Thickness Crack Virgin and Repair Welds in Uniform Thickness Panels Tested at 70°F

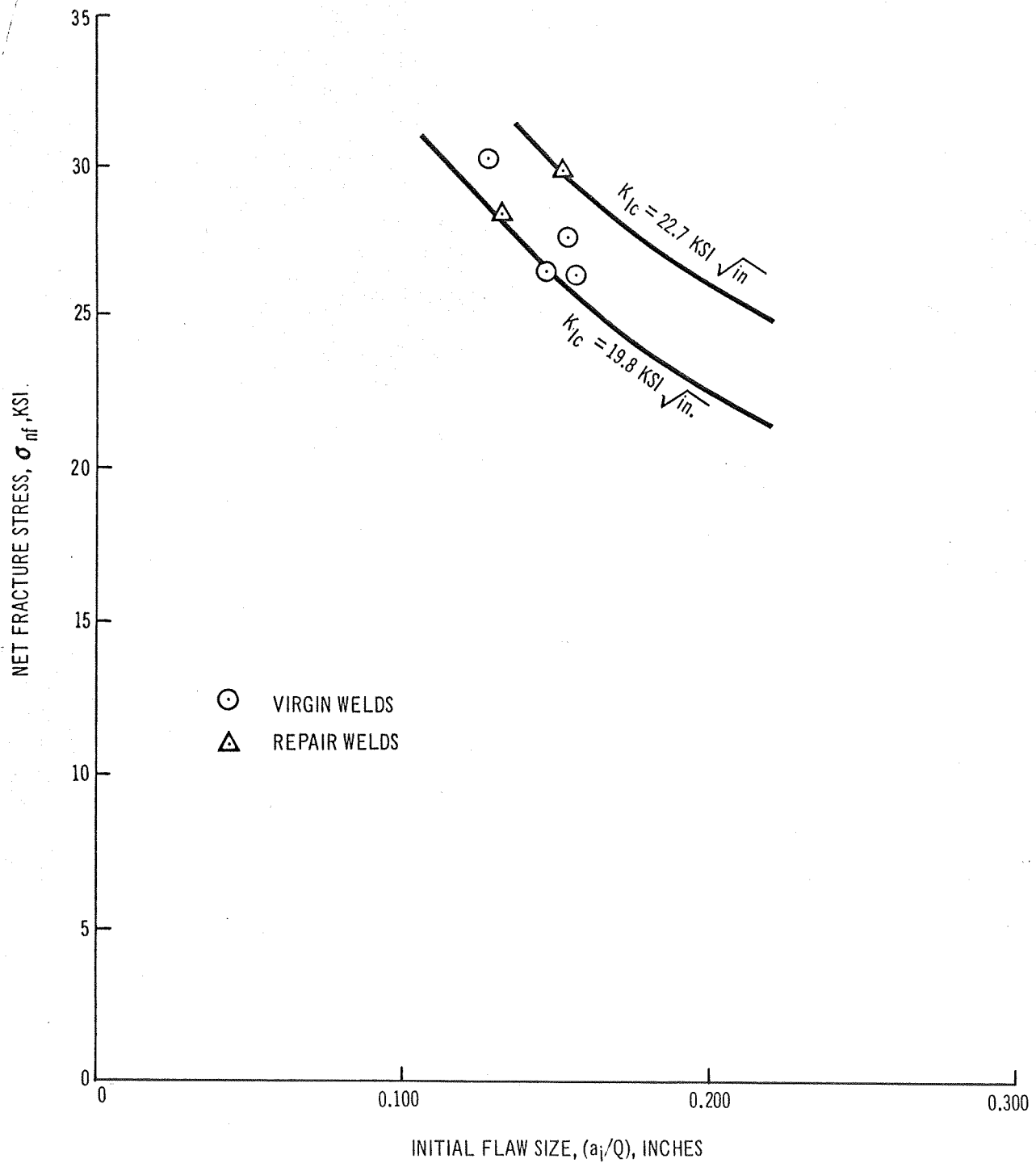


Figure 16. Stress Vs. Flaw Size for Partial-Thickness Crack Virgin and Repair Welds in Uniform Thickness Panels Tested at -320°F After Proof Testing at 70°F

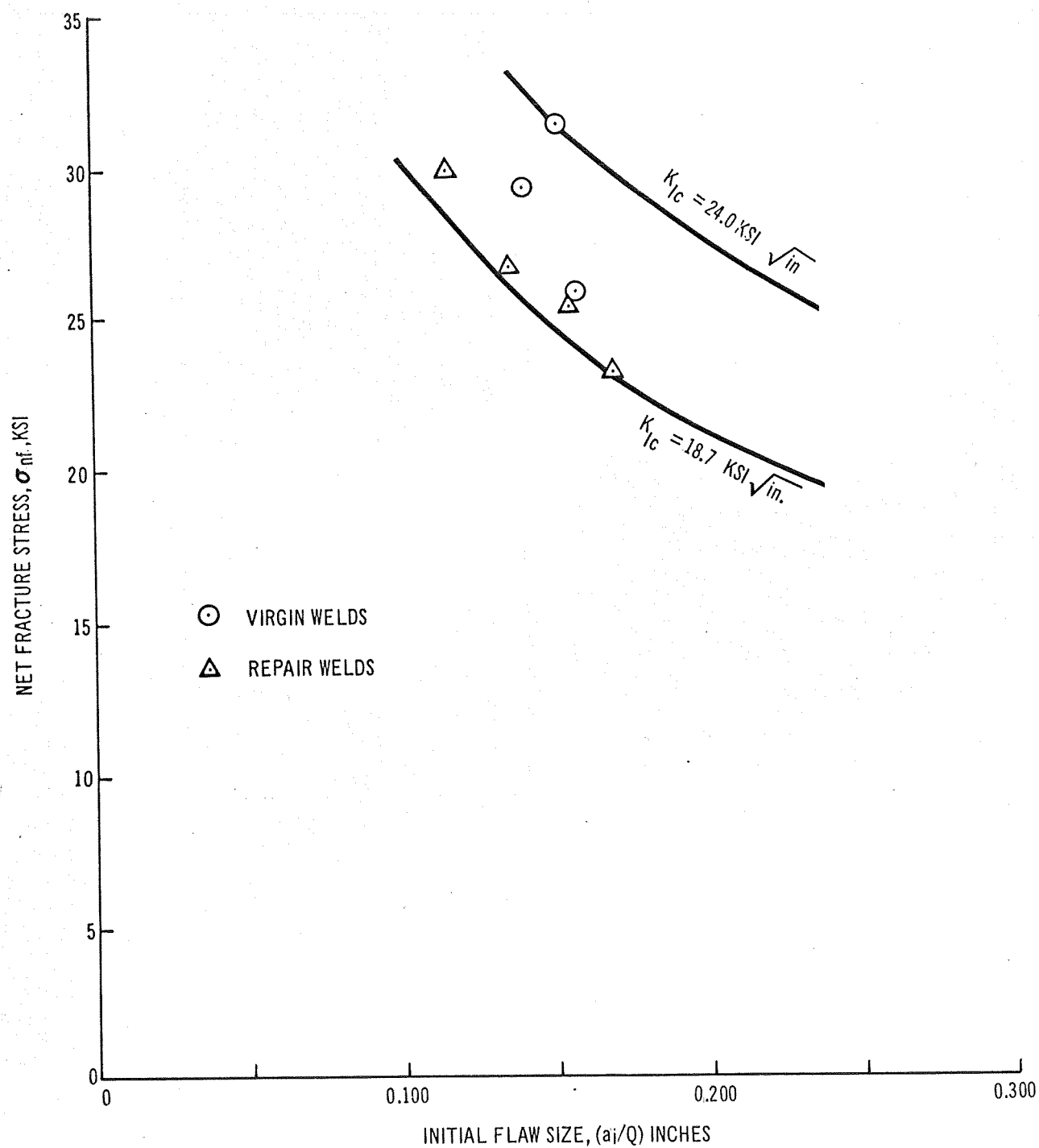


Figure 17. Stress Vs. Flaw Size for Partial-Thickness Crack Virgin and Repair Welds in Uniform Thickness Panels Tested at -320°F Without Prior Proof Testing

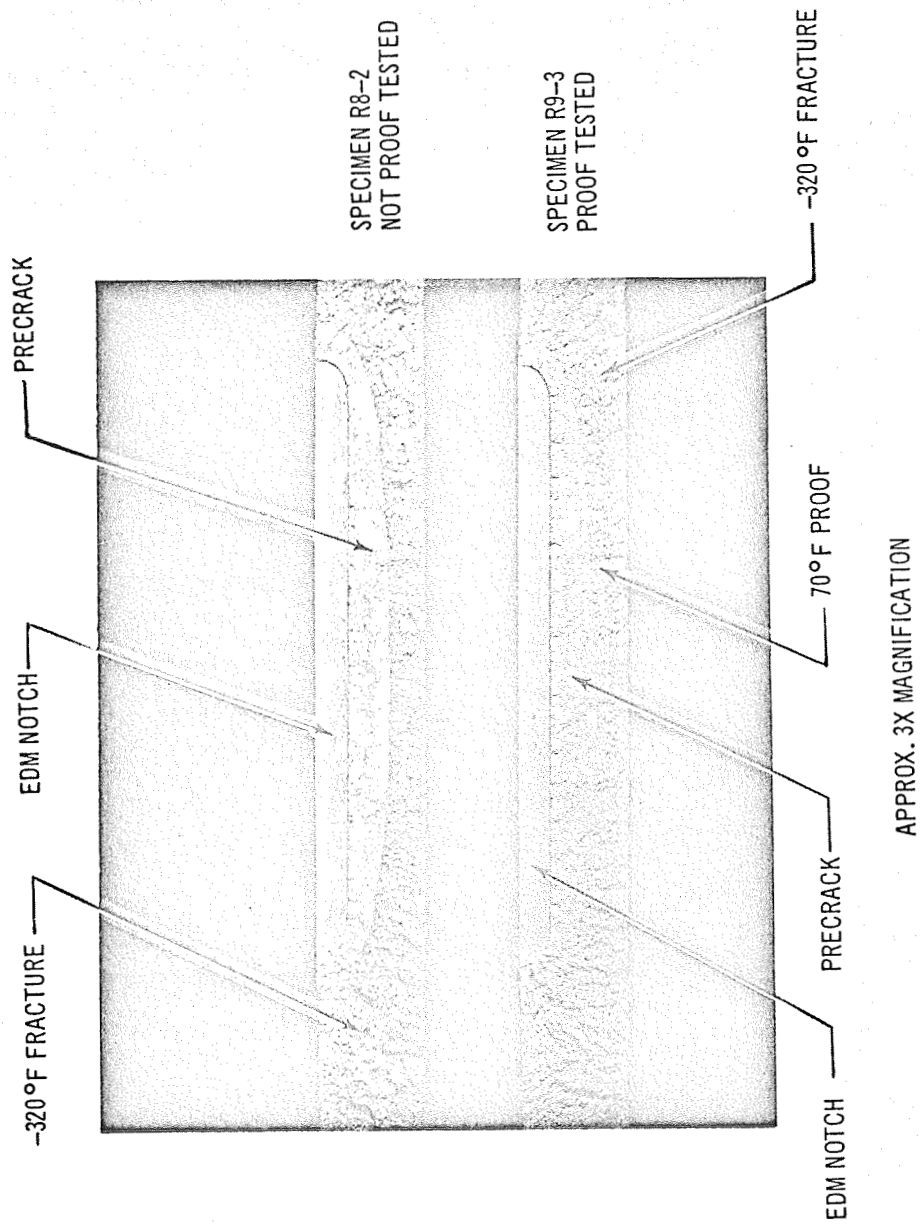


Figure 18. Flaw Growth in Uniform Thickness Welds During Proof Testing

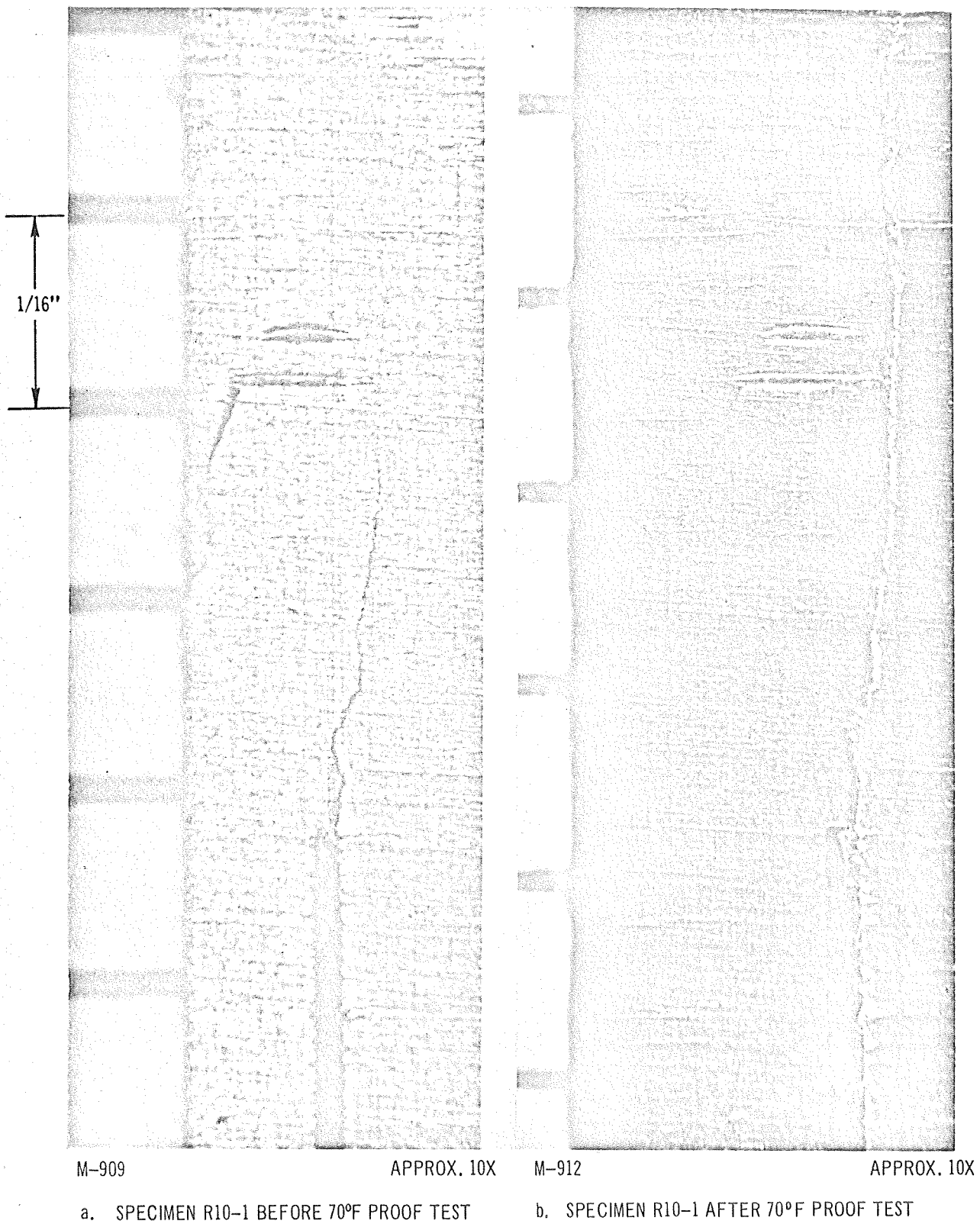


Figure 19. Effect of 70°F Proof Test on Crack Surface Appearance and Growth in Partial-Thickness Crack Specimen (Gaposis)

inspection or ordinary nondestructive testing methods (e.g. penetrant, X-ray) after proof testing.

Static test data from through-cracked 12-inch wide panels are listed in Table 8 together with previous data on 1/8-inch thick TIG-welded 2014-T6 (Reference 3). The data are also plotted in Figure 20. The critical crack length (ℓ_c) was measured by scribing several lines on the specimen perpendicular to and ahead of the cracks and spaced 0.1-inches apart, as shown in Figure 21. As the specimen was loaded, the crack grew and the number of scribe marks intercepted prior to catastrophic failure was noted by observers watching each crack tip. The total amount of growth observed was then simply added to ℓ_o to obtain ℓ_c .

3.2.3 Cyclic Flaw Growth Tests of Meridional Welds

Results of cyclic flaw growth tests of 6-inch wide partial-thickness crack specimens are listed in Table 9. Calculation of stresses, flaw sizes and stress intensities was performed in the same manner as for static tests, described above, except that the flaw dimensions at the beginning of each loading or proof testing cycle were regarded as the initial flaw dimensions for the cycle and, accordingly, were used to calculate (a_1/Q_{nf}) and K_{Ic} values. At the same time, the enlarged flaw dimensions at the end of each cycle were used to calculate the net stress for the cycle. In those cases where flaw growth could not be measured, it was assumed that no flaw growth had occurred during the cycle and the last measureable dimensions were used, enclosed in parentheses in Table 9. No value of

TABLE 8

RESULTS OF STATIC TESTS ON WELDED THROUGH-CRACKED SPECIMENS

Specimen Number	Specimen Width, W (in.)	Specimen Thickness, (in.)	Gross Fracture Stress, σ_g (ksi)	Critical Crack Length, ℓ_c (in.)	Initial Crack Length ℓ_o (in.)	K_{CN} (ksi $\sqrt{\text{in.}}$)	K_C (ksi $\sqrt{\text{in.}}$)
V18-1	12.01	0.189	21.8	3.95	2.54	44.4	57.0
V18-2	12.01	0.189	25.0	2.55	1.57	39.6	51.0
1*	12.00	0.125	18.7	4.88	4.06	49.7	55.8
2*	12.00	0.125	21.9	4.50	3.17	50.4	62.0
3*	12.00	0.125	28.8	2.58	1.69	47.3	59.1

* Reference 3.

TABLE 9

UNIFORM THICKNESS CYCLIC FLAW GROWTH TESTS

SPECIMEN		INITIAL FLAW SIZE			PROOF/CYCLIC LOADING				FLAW SIZE AFTER PROOF/CYCLIC LOADING				K _I		NOTES				
Specimen Number and Type	Width, W (in.)	Thickness at Weld, B, (in.)	Depth, a ₁ (in.)	Length, 2c ₁ (in.)	Shape, a ₁ /2c ₁	Size, a ₁ /a _{1f} (in.)	Loading Cycle Number**	Loading Temp. (°F)	Gross Stress, σ _g (ksi)	Net Stress, σ _n (ksi)	Depth, a _p (in.)	Length, 2c _p (in.)	Slide, λ (in.)	Shape, a/2c (in.)	Size, a/a _{1f} (in.)	Weld F _{ty} (ksi)	Apparent K _{Ig} (ksi√in.)	Apparent K _I (net) (ksi√in.)	
R11-4 6.010 0.193			0.123	0.693	0.177	0.116	P1	70	20.2	21.5	0.128	0.718		0.178	0.121	18.7	13.5	14.4	Cured 64 hours at 160°F after proof test. Re-cracked in flexure before 2nd proof test.
			0.129	0.778	0.165	0.120	P2	70	17.6	19.0	0.136	0.815		0.166	0.126	*	11.8	12.9	
			0.136	0.815	0.166	0.122	1	-320	23.0	(24.9)	(0.136)	(0.815)		(0.166)	(0.122)	31.8	15.6	(17.0)	
			(0.136)	(0.815)	(0.166)	0.125	2	-320	25.0	(27.0)	(0.136)	(0.815)		(0.166)	(0.125)	31.8	(17.1)	(18.6)	
			(0.136)	(0.815)	(0.166)	(0.128)	3	-320	27.1	(29.3)	(0.136)	(0.815)		(0.166)	(0.128)	31.8	(18.7)	(20.5)	
R20-2 6.007 0.188			0.130	1.102	0.117	0.140	P1	70	19.3	22.1	0.153	1.176		0.130	0.161	18.7	14.1	16.1	Failed
			0.153	1.176	0.130	0.146	1	-320	20.5	(23.4)	(0.153)	(1.176)		(0.130)	(0.146)	31.8	15.1	(17.5)	
			(0.153)	(1.176)	(0.130)	(0.146)	2	-320	20.5	(23.4)	(0.153)	(1.176)		(0.130)	(0.146)	31.8	(15.1)	(17.5)	
			(0.153)	(1.176)	(0.130)	(0.146)	3	-320	20.5	(23.4)	(0.153)	(1.176)		(0.130)	(0.146)	31.8	(15.1)	(17.5)	
			(0.153)	(1.176)	(0.130)	(0.146)	4	-320	20.5	(23.4)	(0.153)	(1.176)		(0.130)	(0.146)	31.8	(15.1)	(17.5)	
			(0.153)	(1.176)	(0.130)	(0.147)	5	-320	21.0	27.0	Thru	1.415	0.90	-----	-----	*	(15.5)	(20.2)	
R20-3 6.000 0.190			0.128	1.100	0.116	0.139	P1	70	19.0	21.7	0.155	1.166		0.132	0.162	18.7	13.8	15.8	Failed
			0.155	1.166	0.132	0.147	1	-320	20.3	(23.2)	(0.155)	(1.166)		(0.132)	(0.162)	31.8	15.0	(17.4)	
			(0.155)	(1.166)	(0.132)	(0.147)	2	-320	20.3	(23.2)	(0.155)	(1.166)		(0.132)	(0.162)	31.8	(15.0)	(17.4)	
			(0.155)	(1.166)	(0.132)	(0.147)	3	-320	20.3	(23.2)	(0.155)	(1.166)		(0.132)	(0.162)	31.8	(15.0)	(17.4)	
			(0.155)	(1.166)	(0.132)	(0.147)	4	-320	20.3	(23.2)	(0.155)	(1.166)		(0.132)	(0.162)	31.8	(15.0)	(17.4)	
R20-1 6.001 0.187			0.111	1.062	0.104	0.123	P1	70	19.0	(20.7)	(0.111)	(1.062)		(0.104)	(0.123)	18.7	13.0	(14.2)	Dye-penetrant inspected after proof test. Failed
			(0.111)	(1.062)	(0.104)	(0.123)	P2	70	19.7	(21.5)	(0.111)	(1.062)		(0.104)	(0.123)	*	(13.5)	(14.7)	
			(0.111)	(1.062)	(0.104)	(0.123)	P3	70	23.8	29.4	Thru	(1.218)	0.700	-----	-----	*	(16.3)	(20.2)	
			Thru	1.218	-----	-----	P4	70	24.0	29.7	Thru	(1.218)	-----	-----	-----	*	-----	-----	

* Yield strength not determined; assume F_{ty} = highest net proof stress experienced by the specimen at 70°F, in order to calculate Q and K_I.

** Loaded at approximately 5000 pounds per minute and held at load one minute.

(-) Estimated conservative value.

TABLE 9 (Cont'd)

SPECIMEN		INITIAL FLAW SIZE				PROOF/CYCLIC LOADING				FLAW SIZE AFTER PROOF/CYCLIC LOADING				K _I		NOTES							
Specimen Number and Type	Width, W (In.)	Thickness at Weld, B, (In.)	Depth, a ₁ (In.)	Length, 2c ₁ (In.)	Shape, a ₁ /2c ₁	Size, a ₁ /Q _{nt} (In.)	Loading Cycle Number**	Loading Temp. (°F)	Gross Stress, σ _g (ksi)	Net Stress, σ _n (ksi)	Depth, a _p (In.)	Length, 2c _p (In.)	Slide, λ, (In.)	Shape, a/2c (In.)	Size, a/Q _{nt} (In.)	Weld F _{ty} (ksi)	Apparent K _{Ig} (ksi√In.)	Apparent K _I (net) (ksi√In.)					
R21-3	5.999	0.189	0.148	1.302	0.113	0.161	P1	70	16.4	19.2	0.157	1.340		0.117	0.170	18.7	12.9	15.1	Failed Cured 64 hours at 160°F after proof test. Re-cracked in flexure before 2nd proof test.				
			0.157	1.340	0.117	0.155	1	-320	20.6	(25.9)	Thru	(1.340)				31.8	15.6	(19.9)					
			Thru	(1.340)			2	-320	21.4	(26.9)	Thru	(1.340)				31.8							
V16-3	6.010	0.193	0.115	0.695	0.165	0.110	P1	70	20.2	21.4	0.116	0.708		0.163	0.112	22.2	13.0	13.9	Failed Cured 70 hours at 160°F after proof test.				
			0.120	0.769	0.156	0.113	P2	70	17.7	18.9	0.122	0.789		0.154	0.115	22.2	11.5	12.4					
			0.122	0.789	0.154	0.109	1	-320	20.7	(22.1)	(0.122)	(0.789)		(0.154)	(0.109)	32.6	13.3	(14.3)					
			(0.122)	(0.789)	(0.154)	(0.109)	2	-320	20.9	(22.4)	(0.122)	(0.789)		(0.154)	(0.109)	32.6	(13.4)	(14.4)					
			(0.122)	(0.789)	(0.154)	(0.109)	3	-320	21.1	(22.6)	(0.122)	0.800		(0.152)	(0.110)	32.6	(13.6)	(14.6)					
			(0.122)	(0.80)	(0.152)	(0.110)	4	-320	21.4	(22.9)	(0.122)	0.800		(0.152)	(0.110)	32.6	(13.8)	(14.9)					
			(0.122)	(0.80)	(0.152)	(0.110)	5	-320	21.6	(23.1)	(0.122)	0.800		(0.152)	(0.110)	32.6	(13.9)	(15.0)					
			(0.122)	(0.80)	(0.152)	(0.111)	6	-320	21.9	(23.4)	(0.122)	0.800		(0.152)	(0.111)	32.6	(14.2)	(15.2)					
			(0.122)	(0.80)	(0.152)	(0.111)	7	-320	22.2	(23.8)	(0.122)	0.801		(0.150)	(0.112)	32.6	(14.4)	(15.5)					
			(0.122)	(0.81)	(0.150)	(0.112)	8	-320	22.4	(24.0)	(0.122)	0.802		(0.148)	(0.112)	32.6	(14.5)	(15.7)					
			(0.122)	0.82	(0.148)	(0.112)	9	-320	22.7	(24.3)	(0.122)	0.802		(0.148)	(0.112)	32.6	(14.8)	(16.0)					
			(0.122)	0.82	(0.148)	(0.113)	10	-320	22.9	(24.6)	(0.122)	0.803		(0.146)	(0.113)	32.6	(14.9)	(16.1)					
			(0.122)	0.83	(0.146)	(0.113)	11	-320	23.2	(24.9)	(0.122)	0.803		(0.146)	(0.113)	32.6	(15.2)	(16.4)					
			(0.122)	0.83	(0.146)	(0.114)	12	-320	23.4	(25.1)	(0.122)	0.804		(0.145)	(0.114)	32.6	(15.3)	(16.6)					
			(0.122)	0.84	(0.145)	(0.114)	13	-320	23.7	(25.5)	(0.122)	0.804		(0.145)	(0.114)	32.6	(15.5)	(16.8)					
			(0.122)	0.84	(0.145)	(0.115)	14	-320	24.0	(25.9)	(0.122)	0.808		(0.138)	(0.117)	32.6	(15.8)	(17.1)					
			(0.122)	0.88	(0.138)	(0.117)	15	-320	24.2	(26.1)	(0.122)	0.808		(0.138)	(0.117)	32.6	(16.0)	(17.4)					
			(0.122)	0.88	(0.138)	(0.117)	16	-320	24.5	(26.4)	(0.122)	0.809		(0.137)	(0.118)	32.6	(16.2)	(17.7)					
			(0.122)	0.89	(0.137)	(0.118)	17	-320	24.7	(26.7)	(0.122)	0.890		(0.135)	(0.118)	32.6	(16.4)	(17.9)					
			(0.122)	0.90	(0.135)	(0.119)	18	-320	25.0	(27.1)	(0.122)	0.895		(0.128)	(0.120)	32.6	(16.7)	(18.3)					
			(0.122)	0.95	(0.128)	(0.121)	19	-320	25.3	(27.5)	(0.122)	0.898		(0.124)	(0.122)	32.6	(17.0)	(18.7)					
			(0.122)	0.98	(0.124)	(0.122)	20	-320	25.5	(27.8)	(0.122)	1.00		(0.122)	(0.123)	32.6	(17.2)	(19.0)					
			(0.122)	1.00	(0.122)	(0.123)	21	-320	25.8	(31.0)	Thru	1.07	0.50	Thru	1.07	0.50		32.6		(17.5)	(21.3)		
			Thru	1.07			22	-320	26.0	(32.0)	Thru	1.20	0.87	Thru	1.20	0.87		32.6					
			Thru	1.20			23	-320	25.8	(31.0)	Thru	(1.20)		Thru	(1.20)			32.6					
			V14-3	6.012	0.189	0.129	0.707	0.182	(0.114)	P1	70	(17.7)	(18.9)	0.129	0.707		0.182	(0.114)		22.2	(11.6)	(12.5)	Failed Cured 70 hours at 160°F after proof test.
						(0.129)	(0.707)	(0.182)	(0.112)	(1-100)	-320	(23.7)	(25.3)	(0.129)	(0.707)		(0.182)	(0.112)		32.6	(15.4)	(16.5)	
						(0.129)	(0.707)	(0.182)	(0.121)	(101-200)	70	(23.7)	(25.3)	(0.129)	(0.707)		(0.182)	(0.121)		*	(16.1)	(17.2)	
						(0.129)	(0.707)	(0.182)	(0.110)	(201-300)	-320	(23.7)	(25.3)	Thru	(1.13)	0.82	(0.167)	(0.175)		32.6	(15.4)	(18.8)	
						Thru	1.13			301	70	(23.7)	(22.0)	Thru	(1.365)					*			

* Yield strength not determined; assume F_{ty} = highest net proof stress experienced by the specimen at 70°F, in order to calculate Q and K_I.

** Loaded at approximately 5000 pounds per minute and held at load one minute.

(-) Estimated conservative value.

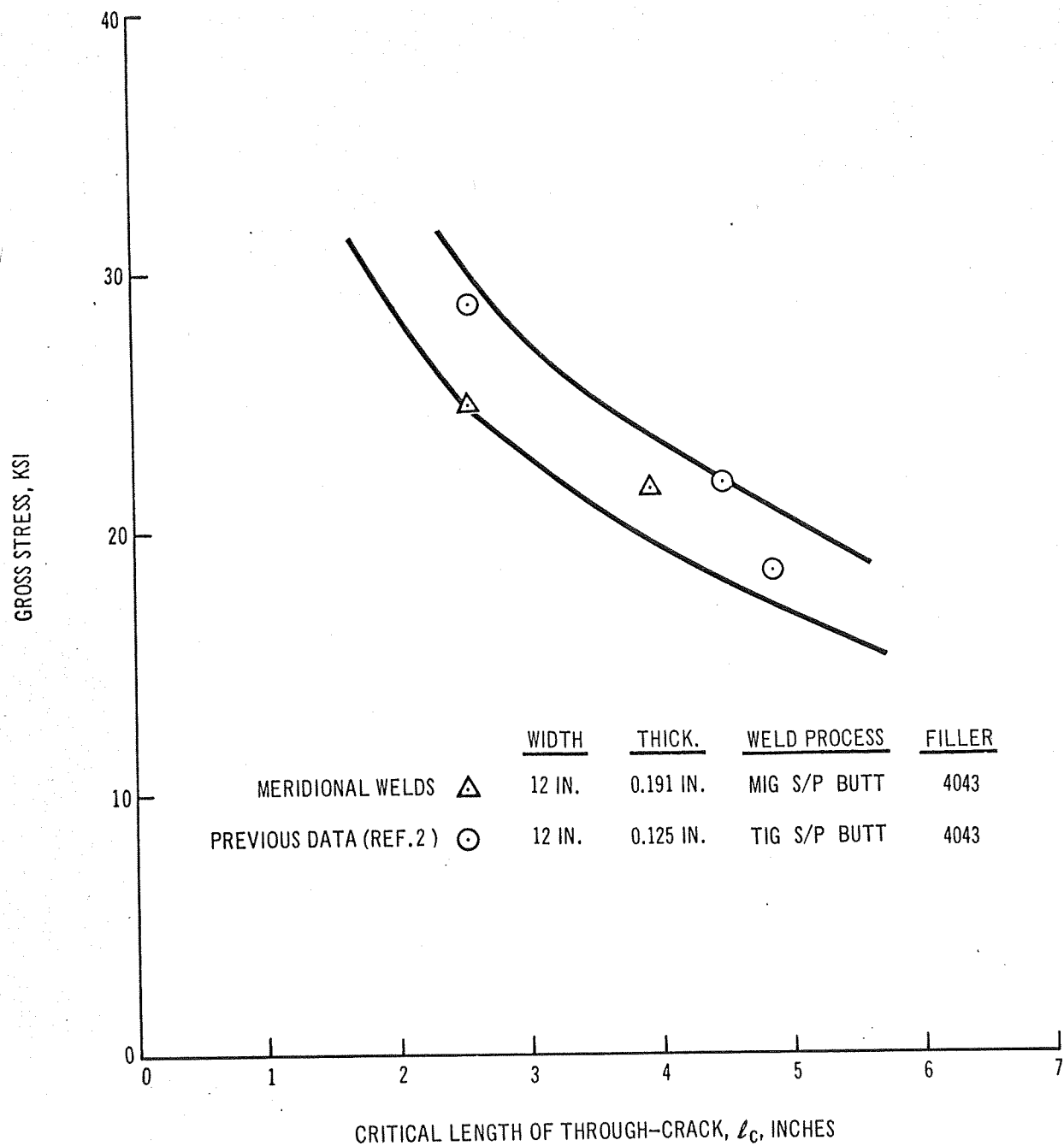


Figure 20. Stress Vs. Critical Length for Through-Cracked Virgin Welds in Uniform Thickness Panels Tested at 70°F

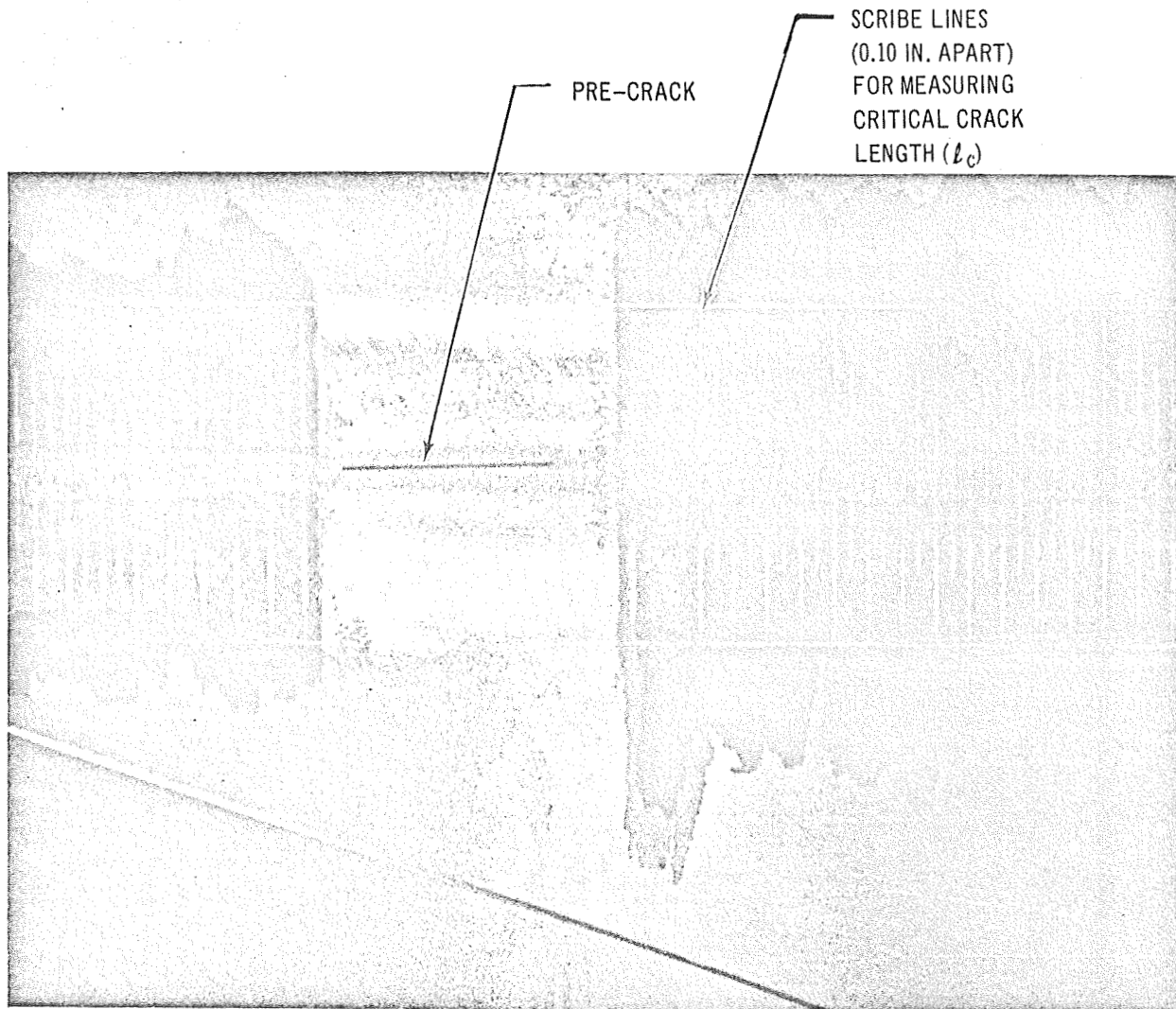


Figure 21. Scribed 12-Inch Wide Through-Thickness Crack Specimen

K_I is reported for cycles for which the crack was initially through the thickness. However, in cases where the partial-thickness crack grew through the thickness during the loading cycle, K_I values are listed, having been based on initial flaw size (in accordance with the calculation procedure for static tests).

4.0 DISCUSSION OF RESULTS

4.1 Flaw Growth in Weld Lands

It had been anticipated from strain gage data on S-IVB weld lands that some flaw growth might occur during proof testing of weld lands containing partial-thickness cracks. The data obtained in this study indicates that a certain amount of subcritical flaw growth can be expected whenever a surface-cracked element is loaded eccentrically in a way which acts to bend open the crack. It has also been demonstrated that extra eccentricity of loading will considerably increase the amount of growth. However, even uniform thickness panels with partial-thickness cracks exhibit flaw growth when loaded, probably due to the bending induced by the presence of the crack on one surface. However, it has also been shown that the strengths of weld lands in which considerable flaw growth has occurred are approximately the same as similar specimens in which cracks have not enlarged and also the same as uniform thickness specimens containing similar partial-thickness cracks. That is, the flaw growth which occurs due to bending apparently does not reduce the net fracture strength of a precracked panel. However, no partial-thickness cracks were placed on the interior (chem-milled) face of the weld lands and the behavior of such cracks is difficult to

predict. On one hand, one would expect that flaws of a certain size or larger would, during loading, grow into regions of progressively higher stresses, causing a rapid and rather abrupt fracture to occur. On the other hand, the crack itself would be located so as to induce bending stresses opposite to the weld land and might therefore be expected to neutralize the bending stresses and grow in a more stable manner. Tests of such interior surface-cracked weld lands would have to be made on sufficiently wide panels to simulate the stress state in a large dome.

4.2 Effect of Test Temperature, Weld Type and Prior Proof Testing on K_{Ic}

The data obtained shows no significant difference between the range of K_{Ic} values for virgin and repair welds at 70°F and -320°F tests. One would certainly expect to find a major test temperature effect and a minor weld type effect in welds containing much smaller flaws, as the fracture stress approaches the ultimate strength of the uncracked material. There is no need, however, to consider fracture stresses so much greater than operating stress.

Proof tested welds were also similar in K_{Ic} and fracture strength to non-proof tested welds, except for one unusually low strength and K_{Ic} for the single weld land specimen which was failed without prior proof testing. Subject to future disproof, that data point is assumed to be erroneous because it alone varies so much from the rest of the data. Lest the data from specimen 6-4 also be taken too much at face value, it should be pointed out that this specimen failed suddenly in the

loading grip holes during an attempt to fail it at -320°F . It was then gripped with rough friction jaws (with poor control of alignment) and failed at 70°F .

4.3 Use of Net Section Stresses

The validity of using net stresses rather than gross stresses for the 6-inch specimen was seriously questioned near the end of the testing program. To demonstrate that net stresses were not unconservative for the 6-inch specimens, two 12-inch wide specimens were prepared with partial-thickness cracks similar to two 6-inch wide precracked specimens which had been tested at 70°F . The gross fracture strength and K_{Icg} values for the 12-inch wide panels agreed completely with the net fracture strength and $K_{Ic}(\text{net})$ values on the 6-inch wide specimens as shown in Figure 22. (All specimens were taken from virgin welds prepared exactly alike on the same production fixture). The use of net section stresses enables one to simulate the behavior of very large tanks with reasonably-sized precracked specimens at a greatly reduced testing cost.

4.4 Leak-Before-Burst

4.4.1 Leak Modes

The growth of a partial-thickness crack through the wall of a tank is classified as a leak if no unstable growth occurs after penetration of the wall. Stable extension of a partial-thickness crack can occur on rising load if sufficient bending is present. Depending on the initial

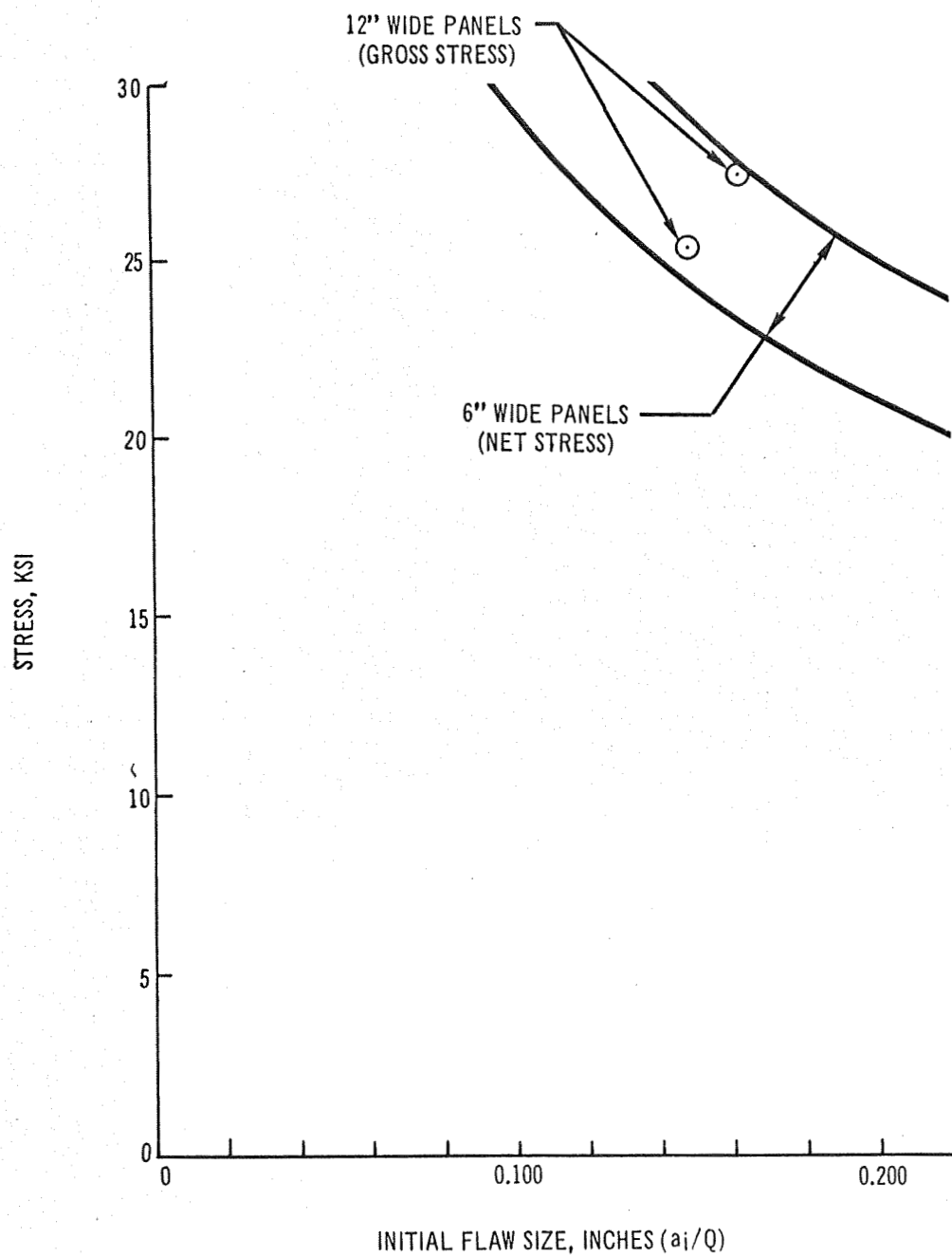


Figure 22. Verification of the Use of Net Stress for 6-Inch Wide Panels

size and shape of the partial-thickness crack, the degree of bending, the maximum applied stress and the total thickness of the wall, the stable extension of the crack may proceed until penetration and leaking occurs. By the time penetration of a relatively thin wall has been completed, the character of the stress field near the crack front has undergone a change from predominantly plane strain to predominantly plane stress. If the maximum length of the penetrated crack is less than the critical length of a through-thickness crack for that stress level, the penetrated crack exists under plane stress stability. Further extension of the penetrated crack would require increased applied stress. On the other hand, if the maximum length of the penetrated crack exceeds the critical length of a through-thickness crack, unstable crack propagation will take place.

Leak can also occur if a partial-thickness crack becomes unstable, propagates and penetrates the wall thickness becoming a through-thickness crack of length less than critical for plane stress instability. Such a crack would arrest after penetration and become stable as a leaking, through-thickness crack. Further extension of the crack would require increased applied stress. If the length of the crack at the time of penetration exceeds the critical length for plane stress instability, unstable propagation would continue.

4.4.2 Evidence for Stable Leak Conditions

Stable penetration of the thickness by an initially partial-thickness crack was observed in a number of specimens tested in this program. In most of these specimens, the leak was detected after proof testing; the stress level at which penetration took place was not observed. In the two 12-inch wide partial-thickness crack specimens statically tested at 70°F, observers detected penetration at a stress level well below the fracture stress.

In reviewing the test results it was observed that the initial depth of partial-thickness cracks which did not penetrate the thickness during proof loading was never greater than about 0.150-inch. All partial-thickness cracks having initial depths of about 0.154-inch, or greater, penetrated the thickness during proof testing at 70°F. Sufficient data were not obtained to make a complete analysis of conditions conducive to stable leak. However, based on the observations made during this test program, it appears that partial-thickness cracks in the meridian weld of the LOX dome, having an initial depth equal to or greater than 80% of the weld thickness, can penetrate the wall in a stable manner and leak during proof test without causing catastrophic fracture of the tank. The minimum length of such stable, leaking cracks is not known; the maximum length, however, based on the minimum fracture toughness of 12-inch wide through-crack specimens (Figure 20), is 4.4-inches. Application of plane stress data from 12-inch wide panels to a large structure such as the S-IVB is extremely conservative since the critical

length of through-thickness cracks is strongly dependent on specimen geometry and is known to increase with increasing width. Nevertheless, if these data could be applied directly to the meridian weld of the LOX dome, they would indicate that through-thickness cracks longer than 4.4-inches would result in catastrophic fracture at the proof stress level.

It was noted above that no temperature effects between 70°F and -320°F were observed on the fracture toughness of the welds as determined with partial-thickness crack tests. Assuming that the same observation would be made for through-thickness crack tests, the data obtained at 70°F could then be applied to operating conditions for the LOX tank. Again applying the 12-inch wide specimen data directly to the LOX dome meridian welds and ignoring width effects, through-thickness cracks longer than 2.55-inches would result in catastrophic failure at the maximum operating stress.

4.5 Assessment of Safety of LOX Dome Weldments

The minimum degree of safety of the meridian welds in the LOX dome can be assessed by considering minimum toughness at maximum operating stress and disregarding the very conservative nature of available through-thickness crack data.

The lower bound of all data obtained from all specimens tested under all conditions (Figure 23) provides a critical value of a_1/Q at operating stress of 0.134-inch. In Figure 24 the various combinations of crack depth and crack length which characterize an a_1/Q of 0.134-inch are

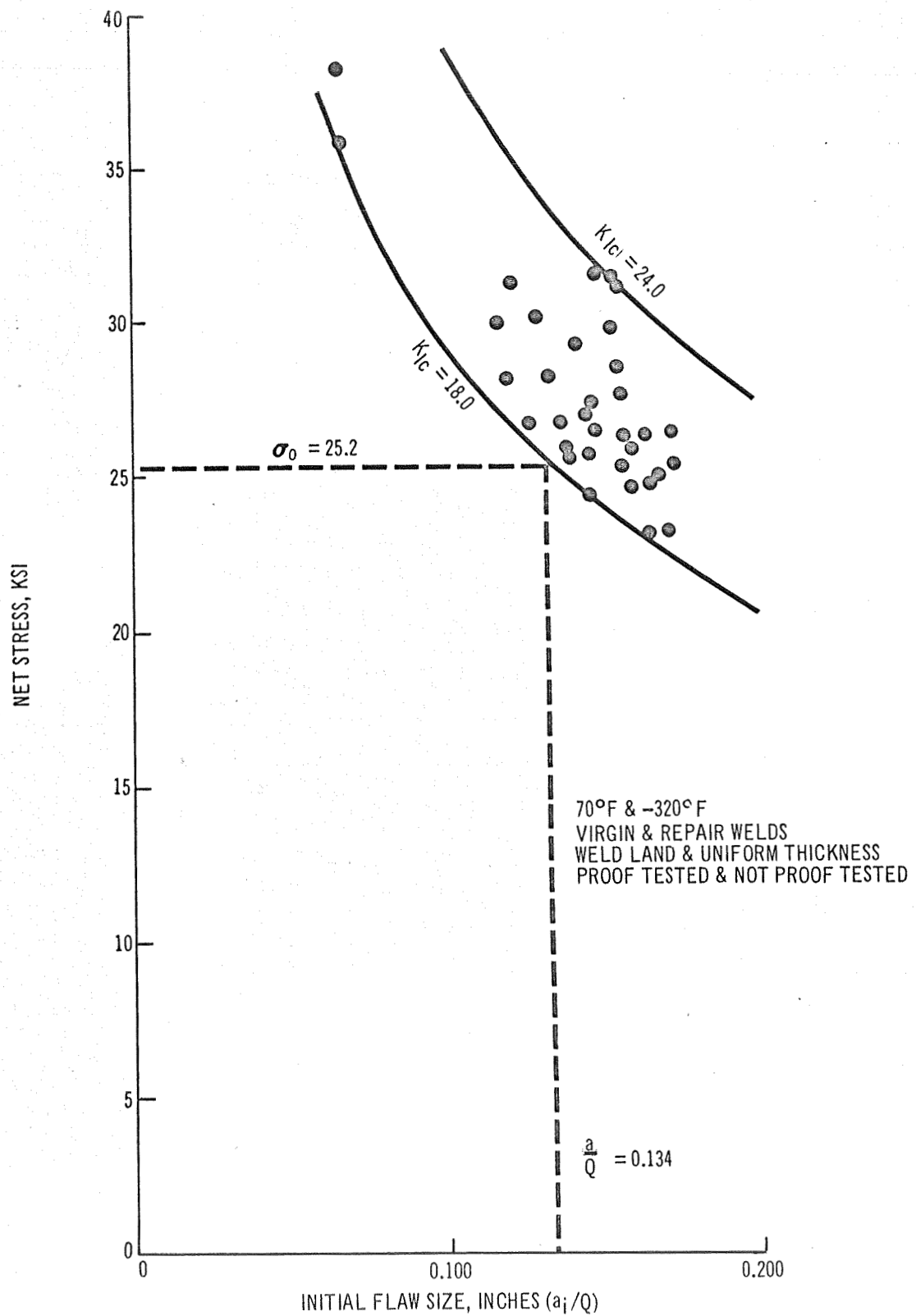


Figure 23. Data Bands for all Static Tests of Partial-Thickness Crack Specimens

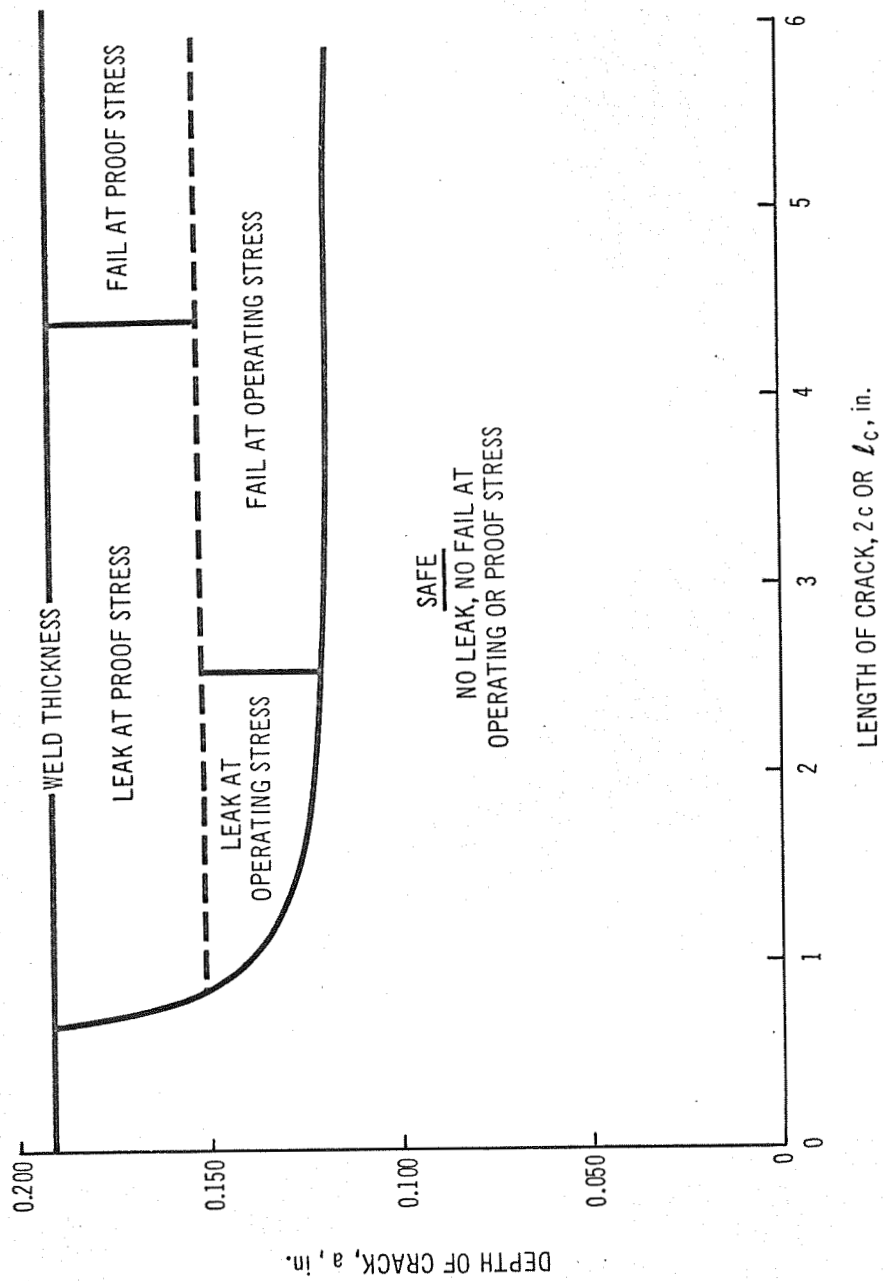


Figure 24. Effect of Cracks on S-IVB Lox Dome Meridian Welds at Proof and Operating Stresses

plotted. Based upon a value of a_1/Q of 0.134-inch, all initial partial-thickness cracks, the dimensions of which fall below the curve in Figure 24, are stable at the operating stress; those cracks above the curve would result in failure of the LOX tank.

However, some of the very deep (deeper than about 80% of the weld thickness) partial-thickness cracks would penetrate the thickness during proof test. If the penetrating cracks were longer than 4.4-inches, failure of the tank would have occurred at proof stress. If the penetrating cracks were shorter than 4.4-inches, a stable leak would have occurred and would have been detected either in proof test, during inspection after proof test, or during the leak check. Such leaks would have been repaired. As a consequence, all cracks above the dashed line in Figure 24 would have been discovered before the tank became operational.

A partial-thickness crack having a depth in the range of 62% to 80% of the weld thickness could survive the proof test without leaking or fracturing as evident in Figure 24. However, the plastic tensile strain imparted to the weld metal near the periphery of such a crack during proof test would result in a permanent displacement of the crack surfaces (gapping) after release of the proof pressure, making penetrant inspection considerably more sensitive. All cracks exhibiting gapping are therefore detectable by standard post-proof inspection procedures. If a crack, 62% to 80% through the weld, somehow should escape post-proof inspection, it could become unstable at the operating stress and penetrate the weld thickness. If the length of the penetrating crack were less than 2.55-inches, the crack would be arrested and would constitute a stable leak. If the length of the penetrating crack were greater than 2.55-inches, the

penetrating crack could be unstable in plane stress and could result in failure.

These considerations are listed in Table 10.

5.0 CONCLUSIONS

As a result of analyzing data produced by tests conducted in this program and considering only minimum toughness as the worst case, the following conclusions can be stated:

Regarding the test data:

1. Negligible differences exist in the fracture toughness of virgin and repair welds in 2014-T6 at 70°F and -320°F
2. Proof testing at 70°F has little influence on the fracture toughness of virgin and repair welds tested at -320°F.
3. Depending upon the degree of bending, the initial depth of the partial-thickness crack, and the applied stress, stable extension of cracks can occur on rising load. Depending on the thickness of the section, the stable extension can result in a leak. Stable extension occurring on one loading cycle has no detrimental effect on the fracture strength observed in a subsequent load cycle.
4. For tests of narrow panels containing large partial-thickness cracks, the use of net stress is advisable in analyzing the results to avoid over-conservatism.

TABLE 10

SUMMARY OF EFFECTS OF CRACKS IN
S-IVB LOX DOME MERIDIAN WELDS

<u>PRE-EXISTING CRACK</u>		Effect of Proof Stress	Effect of Operating Stress
Length, in.	Depth, in.		
Up to 2.5	0 to 60% of Thickness	Gaposis**	No Effect
	60% to 80%	Gaposis**	Leak
	80% to 100%	Leak	*
2.5 to 4.4	0 to 60%	Gaposis**	No Effect
	60% to 80%	Gaposis**	Fail
	80% to 100%	Leak	*
Over 4.4	0 to 60%	Gaposis**	No Effect
	60 to 80%	Gaposis**	Fail
	80% to 100%	Fail	*

* This case not possible (crack detected in proof or leak check).

** Permanent increase in crack opening (See Figure 19).

Regarding proof test of the S-IVB LOX dome meridian welds:

1. Partial-thickness cracks having a depth greater than about 80% of the weld thickness can leak during proof test if the crack length is less than 4.4-inches. If the crack length is greater than 4.4-inches, a crack deeper than 80% of the weld thickness can result in failure during proof test.
2. Partial-thickness cracks having a depth less than about 80% of the weld thickness will not leak or cause failure during proof test.
3. Partial-thickness cracks less than 80% of the weld thickness or leaking cracks which survive proof testing can readily be detected by standard post-proof testing including visual inspection, penetrant inspection or leak testing.

Regarding operating conditions for the S-IVB LOX dome meridian welds:

1. Partial-thickness cracks in LOX dome meridian welds having a depth less than 62% of the weld thickness which survive proof test and post-proof inspection without detection cannot leak or cause failure during service at the maximum operating stress.
2. Partial-thickness cracks having a depth between 62% and 80% of the weld thickness which survive proof test and post proof inspection can penetrate the thickness and become a stable leak if the length of the crack does not exceed 2.55-inches. If the crack length is greater than 2.55-inches, the penetrating crack can result in failure of the LOX dome at the maximum operating stress.

Regarding the conservatism of conclusions drawn from analysis of results of narrow panel tests as applied to large scale structures:

1. A large degree of bending exists in full scale dome welds thus promoting stable extension of partial-thickness cracks therein, leading to the formation of leaks. Similar bending in narrow flat panels (particularly those of uniform thickness) must be less severe. It is therefore reasonable to conclude that the 80% depth requirement for leaks in a full scale dome weld is too conservative and that leaks occur much more readily in full scale domes than in flat test panels.
2. The critical through-thickness crack length of narrow panels at a given stress level is less than the critical length of wider panels or of full scale domes. It is therefore reasonable to conclude that the maximum length of stable leaking cracks in a full scale dome is greater than in narrow (12-inch) panels and that the failure condition for penetrating cracks exceeds the overly-conservative estimates of 4.4-inches for proof stress and 2.55-inches for operating stress.
3. The premise that partial-thickness crack depths in the range 62% to 80% of the thickness and greater than 2.55-inches long can survive post-proof inspection after plastic displacement (gapisis) due to proof loading is not overly conservative provided there is a location in the full scale dome where

post-proof inspection of the meridian welds is not possible. No such location exists in the S-IVB LOX dome and it is therefore reasonable to conclude that this premise is overly conservative.

6.0 RECOMMENDATION

In view of the evidence supporting the likelihood of leak-before-burst at maximum operating stress and of the highly conservative nature of this analysis, it is recommended that alteration of current proof test and operating conditions for the S-IVB LOX dome not be considered.

7.0 REFERENCES

1. ASTM Committee on Fracture Testing of High Strength Materials, "Progress in Measuring Fracture Toughness and Using Fracture Mechanics", Materials Research and Standards, March, 1964.
2. W. F. Brown, Jr., and J. E. Srawley, Plane Strain Crack Toughness Testing of High Strength Metallic Materials, ASTM Special Technical Publication No. 410, 1966.
3. R. H. Christensen, M. S. Tucker, and K. R. Wilson, Crack Propagation Resistance of High-Strength Aluminum Alloys, Douglas Report No. SM-48401, dated July, 1965.

APPENDIX A

NONDESTRUCTIVE METHOD OF DETERMINING FLAW DEPTH

For the greater portion of tests in the test program it was desired to test specimens containing flaws of a precise pre-selected size. During flexural pre-cracking, optical means were used to measure crack length in order to terminate the operation when the crack had grown to within a few thousandths of an inch of the desired length. It was not possible, however, to predict accurately the crack depth achieved in the pre-cracking operation. This could only be accomplished by measuring the flaw dimensions on the fracture surface after mechanical testing.

X-ray, an excellent qualitative, nondestructive test for cracking, was not suitable for making crack depth determinations. Therefore, an alternate nondestructive test was sought which could provide quantitative data relating to flaw depth prior to specimen testing. The method employed consisted of taking eddy current readings both in the area of the flaw and in sound weld metal, using the F. W. Bell Model 1090 Magnetic Reaction Analyzer (MRA) which has been described elsewhere (Reference A-1). Later, following mechanical testing, actual flaw depth was measured and was plotted against the MRA reading to generate a curve for flaw depth vs. MRA reading.

The difference between crack and sound weld MRA readings, and the corresponding crack depth measurements from the several virgin and double repaired weldments are plotted in Figure A-1.

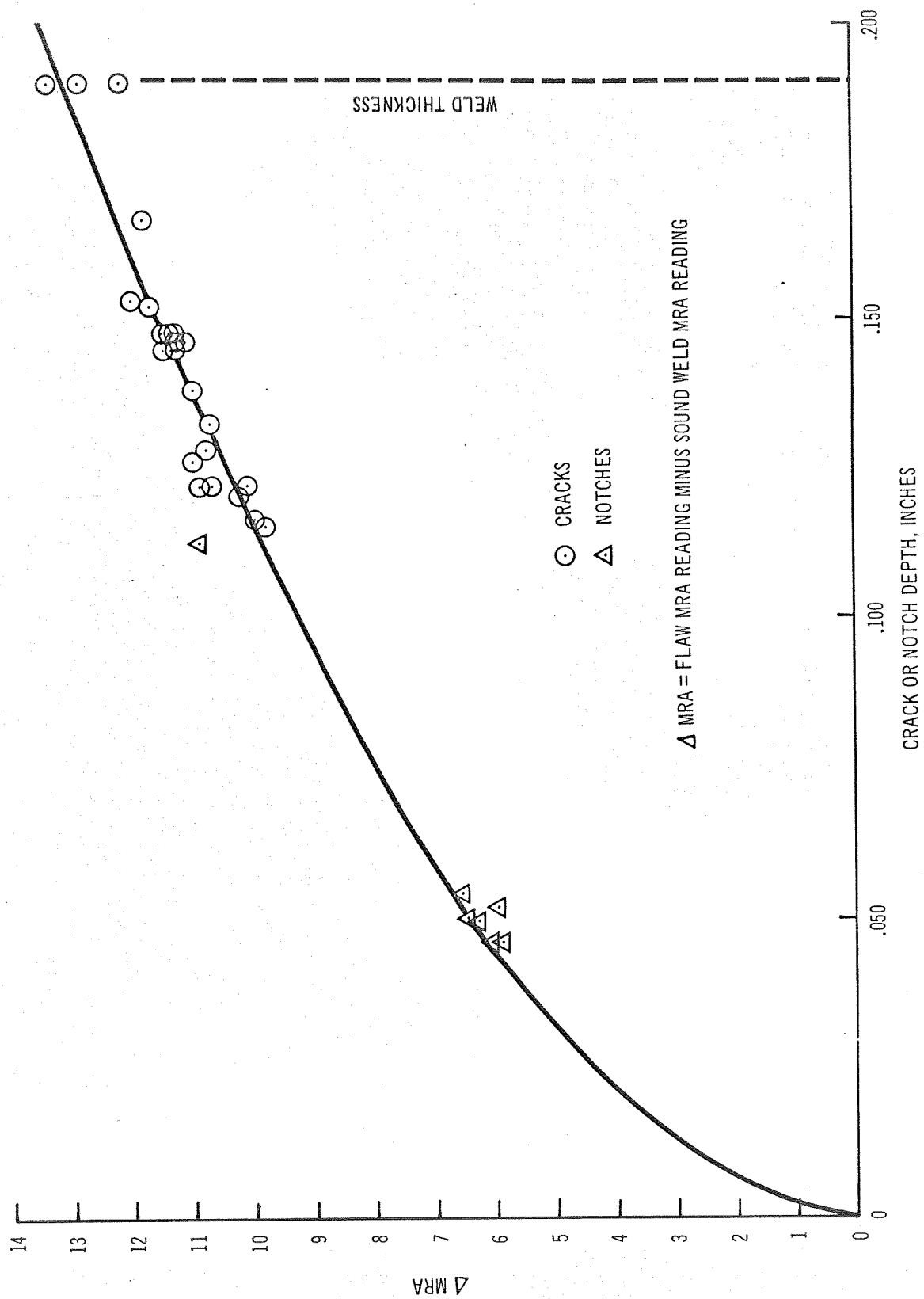


Figure A-1. MRA Data for Notched and Cracked Virgin and Repair Weld Panels

This effort was only partially successful in providing a quantitative nondestructive test of crack depth. Considerable scatter in test data was observed. Particularly, in the deep flaw region (0.120 to 0.180-inches), the range of flaw sizes most often used in this study, the data exhibit the most scatter. In this region crack depth could be predicted to an accuracy of only ± 0.020 -inch. In the shallow flaw range, under 0.100-inch, where the curve is flatter, a sufficient number of specimens were not available to accurately establish the MRA reading scatter band.

Scatter in test data was due to several factors, most of which are known, and which can be accounted for with sufficient testing. Weld metal chemistry changes alter the MRA readings whether a flaw is present or not. Obviously, repaired welds, which contain greater and, perhaps, more widely varying amounts of 4043 (5 per cent silicon) filler alloy will give MRA readings different from virgin welds. Changes in the metallurgical structure of the weld deposit can also produce changes in MRA readings. Such changes may occur as the result of the history of a particular specimen. Proof testing, for example, can cause varying degrees of yielding of the weld deposit, depending on the stress level and the chemistry (virgin/repair) of the weld deposit. Thermal treatments, too, such as the 160°F, 70 hour cure that several of the specimens were given, may well affect the MRA readings. Crack or notch opening further influences MRA readings. The EDM notches were machined to a gap of from 0.005 to 0.010-inch. Again, proof testing, which tends to open flaws may

further affect the MRA readings. Finally, material thickness variations, possibly caused by variations in the weld shaving operation, will also produce differences in MRA readings. None of the above variables, with the exception of notches versus cracks were considered in this effort. Other factors which may have significantly affected test scatter are possible inconsistencies in calibration and set-up of the apparatus and, particularly, operational difficulty in holding the probe tip on the irregular panel surfaces.

In order to utilize effectively the eddy current test method of non-destructively determining flaw depth additional experimentation will be required. More data is particularly needed in the shallow flaw range. It will be necessary to develop correction factors for each of the several variables which are known to influence eddy current readings. As an alternative, it may be preferable to generate crack depth vs MRA value curves for each alloy, material thickness, and environmental history under which specimens may be tested. Feasibility of the method has been demonstrated.

Reference:

- A-1. W. W. Reinhardt, "Nondestructive Thickness Measurement of Dyna-Therm Coatings", Douglas Report DAC 59588, to be published 1968.



*MISSILE & SPACE SYSTEMS DIVISION/SPACE SYSTEMS CENTER
5301 BOLSA AVENUE, HUNTINGTON BEACH, CALIFORNIA*

A DIVISION OF DOUGLAS AIRCRAFT COMPANY, INC.